NOx Emissions and Engine Performance Results for Studied Engine Concepts including final Summary

ULF TENGZELIUS

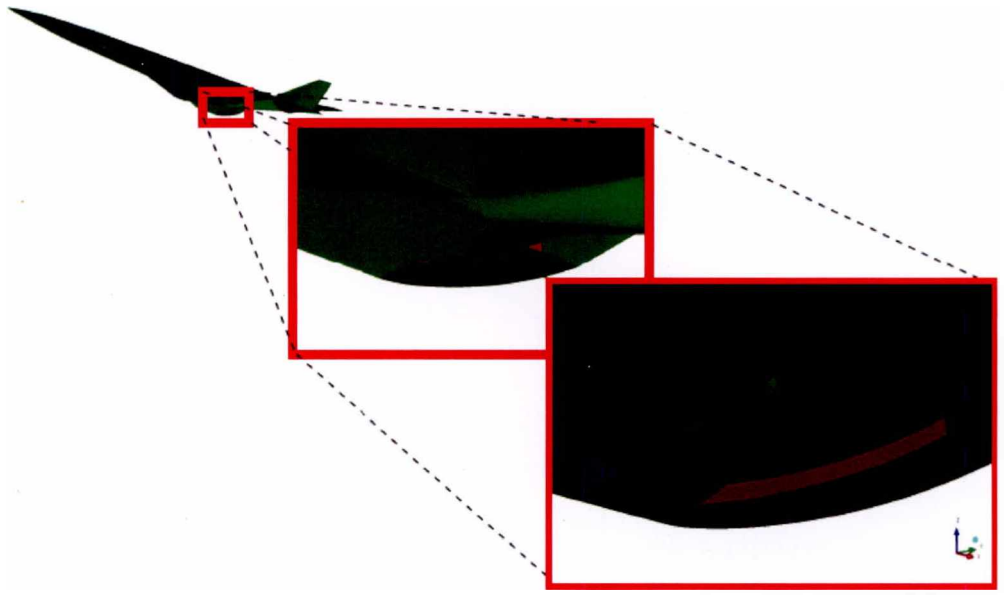

FOI-R--3026--SE Technical report
ISSN 1650-1942 September 2010

Defence & Security, Systems and Technology

Ulf Tengzelius

NOx Emissions and Engine Performance Results for Studied Engine Concepts including final Summary

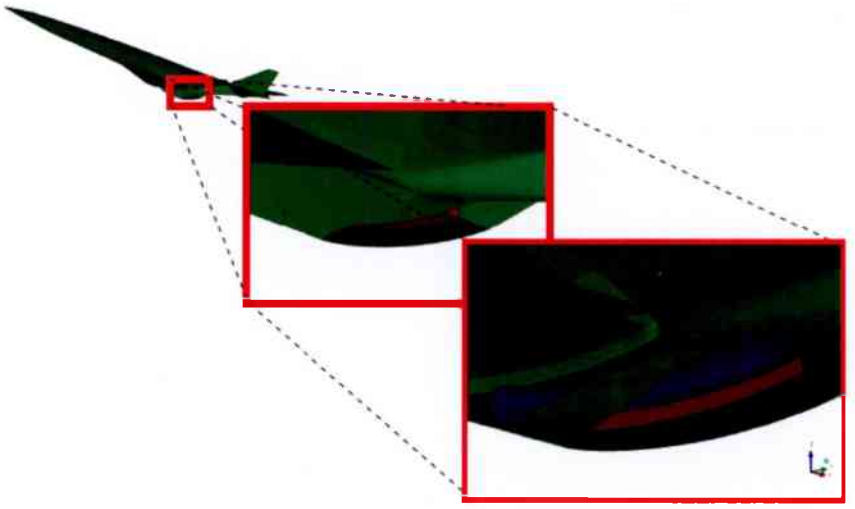

Titel	-
Title	NOx Emissions and Engine Performance Results for Studied Engine Concepts including final summary
Rapportnr/Report no	FOI-R--3026--SE
Rapporttyp/Report Type	Teknisk rapport/Technical report
Sidor/Pages	73p
Månad/Month	September
Utgivningsår/Year	2010
ISSN	ISSN 1650-1942
Kund/Customer	EU 6e ramprogrammet/ FM
Projektnr/Project no	B66013
Godkänd av/Approved by	Marlene Johansson

FOI, Totalförsvarets Forskningsinstitut
Avdelningen för Försvars- och säkerhetssystem
Flyg- och Systemteknik
164 90 Stockholm

FOI, Swedish Defence Research Agency
Defence & Security, Systems and Technology
Aeronautics and Systems Integration
SE-164 90 Stockholm

Sammanfattning

I EU projektet ATLLAS (*Aerodynamic and Thermal Load Interactions with Lightweight Advanced Materials for High Speed Flight – EU 6:e ramprogrammet)* har konceptstudier på RAM-jet drivna överljudsflygplan genomförts. Kärnverksamheten inom projektet låg på studier av lätta, värmetåliga material men också miljöaspekter som buller och emissioner ingick i arbetet. I denna rapportbehandlas emissionsfrågor.

Möjligheten till framtida överljudsflygplan, framdrivna av RAM-jets, aktualiserar frågor om hur atmosfären kan påverkas av avgasutsläpp (emissioner). Frågan gäller främst NOx och dess inverkan på ozonskiktet. Med de flygplanskoncept, Mach 6 och Mach 3, som studerades inom ATLLAS avges förbränningsprodukter på väsentligt högre höjder än för dagens flygtrafik. På ca 25 km:s höjd d.v.s. i de lägre delarna av stratosfären, mot dagens trafik som ligger i de övre delarna av troposfären, på ca 10 km:s höjd.

Rapporten innehåller en litteraturstudie som täcker in NOx- och ozonproblematik, samt motorkoncept. Vidare redovisas grundläggande studier av typiska cruise-NOx nivåer från flygplanskoncepten i ATLLAS satta i relation till möjlig framtida NOx reglering.

Nyckelord:

Emissions, NOx, ozone layer, RAM-jet, SST, Supersonic transporter, stratospheric flight, Överljudsflygplan, Emissioner, ozonlager

Summary

In the cooperative EU project ATLLAS (*Aerodynamic and Thermal Load Interactions with Lightweight Advanced Materials for High Speed Flight – EU 6 th framework)* conceptual studies on supersonic transporters (SST) equipped with RAM-jets have been carried out. The main focus within the project was lightweight heat resistive materials, but also environmental aspects such as gas emissions and noise constituted part of the work. This report covers the emissions.

The possibility of future RAM-jet SST's at high altitude cruise heights actualise matters of atmospheric changes due to exhaust gas emissions. The primary task regards NOx and whether it might threaten the ozone layer. With the aircraft concepts studied within ATLLAS - one Mach 6 and one Mach 3 concept – combustion products are emitted at considerably higher altitudes than for the aircraft fleet of today. This is at altitudes around 25 km's, i.e. in the lower stratosphere, compared to today's traffic which is found in the higher troposphere, around 10 km's above sea level.

The report contains a literature study covering atmospheric NOx / ozone layer matters and low-NOx engine concepts as well as fundamental studies of cruise NOx levels for the conceptual ATLLAS aircraft. The results are related to possible future NOx limitations.

Keywords:

Emissions, NOx, ozone layer, RAM-jet, SST, Supersonic transporter, stratospheric flight, Överljudsflygplan, Emissioner, ozonlager

Table of contents

List of Abbreviations and Symbols

AFR	Air to Fuel Ratio (=1/f, fuel to air ratio)
CEA	The Gordon Mc Bride Chemical Equilibrium Analysis code
EINOx	Emission Index for NOx in grams/kg. Given as grams of NOx ($NO+NO_2$) produced (in grams) divided by amount of fuel (in kg) burnt. The weight of NOx accounted for with mole weight of NO_2 since NO under most circumstances shortly after emission reacts with oxygen in the atmosphere to produce NO_2. EINOx facilitate simple means for estimates of total NOx emissions for an aircraft knowing the fuel consumed. It is also the most used property when NOx emissions for a specific engine/aircraft is to be quantified. It is thereby also valuable for direct comparisons between engines/aircraft .
f	fuel to air ratio (=1/AFR)
fs	stoichiometric fuel to air ratio
HPC	High Pressure Compressor
LPC	Low Pressure Compressor
LTO	Landing – Take Off cycle
M3T	ATLLAS project Supersonic Transport Aircraft concept designed for cruising speeds around Mach 3
M6T	ATLLAS project Supersonic Transport Aircraft concept designed for cruising speeds around Mach 6
NOx	sum of nitrogen oxides NO and NO_2
ppbv	parts per bilion, volume, i.e. one part in 10^9 per volume
pptv	parts per trillion, volume, i.e. one part in 10^{12} per volume
RQL	Rich burn –Quench – Lean burn a common combustion method in modern gas turbine engines to reduce NOx by avoiding burning at equivalence ratios close to 1 where maximum NOx will be generated. First a Rich fuel/air mix is burnt in a primary zone, then these combustion products (containing unburnt fuel) are mixed and cooled with bypassed inlet air. This mix is then combusted in a secondary combustion zone.
SST	Super Sonic Transporter
wEINOx	$wEINOx = h_{kerosene}/h_{H2}*EINOx$ where: h=heating value $h_{kerosene}$=43 MJ/kg (heating value kerosene)

h_{H2}=121 MJ/kg (heating value hydrogen)
$h_{kerosene}/h_{H2}$=0.355 (scale factor between wEINOx and EINOx)

(wEINOx is defined, and used, in this work in order to enable direct comparisons with aircraft engines using hydrogen instead of kerosene as fuel. In wEINOx, the "w" denotes "weighted EINOx", which means that the higher energy value of hydrogen, compared with kerosene, has been included by a factor of around 1/3 which is more relevant for direct EINOx comparisons with aircraft fuelled with kerosene.)

Greek Symbols

$\varnothing$	Equivalence Ratio $\varnothing$ = f/fs where: fs = stoichiometric fuel to air ratio f = actual fuel to air ratio
η_c	engine inlet compression efficiency
η_o	engine over all efficiency
η_{th}	engine thermal efficiency
η_p	propulsive efficiency

1 Introduction

1.1 Scope of the report

The matter of NOx emissions from future SST's of the ATLLAS kind are studied and discussed. This involves a Mach 6 Transport Vehicle concept (denoted M6T) cruising at an altitude of 27 km at M=6, i.e. in the lower stratosphere, and a Mach 3 concept (denoted M3T) cruising at a lower altitude, 23 km. Both vehicles are equipped with combined cycle RAM-jet engines, working in a turbo jet mode for the LTO-cycle and RAM-jet mode in cruise. Knowing the strong NOx production increase with temperature, the M6T with combustor inlet temperatures around 1500 K, clearly makes effective NOx reduction methodologies essential. The M3T, because of its more unconventional RAM-jet principle (if one may speak about "conventional RAM-jets") giving a very large engine air through-flow and a smaller temperature rise, plus the lower free-stream total temperature at Mach 3, can be envisaged as a milder NOx generator.

The report starts with an attempt to summarise the current scientific knowledge of NOx influence on the atmosphere with focus on the ozone layer. The risk for ozone layer depletion has governed the direction of the work into the cruise phase of the flight cycle. Possible future NOx regulation levels are also discussed. It should here be noted that NOx emissions in the stratosphere are, according to the current understanding, more critical for the ozone layer than if they would occur in the troposphere (as for the subsonic fleet of today).

Future and already in-use methodologies for NOx reduction are outlined and some of them are studied a bit more in detail, with attempts to judge their applicability for RAM-jets.

The engines in ATLLAS are treated as "black boxes" in the sense that the detail configuration of burners and combustion chambers are deliberately omitted, this since it falls outside the main scope of the project[1].

The combustion and NOx prediction methods applied in the work are chemical equilibrium and kinetics methods solely. By this restriction one can not expect to get "exact" results for specific engines with in detail defined configurations and working conditions, but the approach is regarded to enable identification of mechanisms and trends from which general conclusions could be drawn. Moreover, this simulation approach is in accordance with the "black box" concept with settled initial state conditions as starting points.

[1] The main scope of ATLLAS could be summarised as (in line with the title):
"aero-thermal loads and advanced materials"

1.2 Results

The atmospheric science of today states that there is a strong risk for ozone depletion from NOx emitted in the stratosphere, but more research in specific fields are needed in order to fully understand the governing mechanisms and to better quantify these risks.

There are not yet any NOx regulations limits established for cruise flight, neither for sub- or supersonic air traffic (airplane emissions are up today only restricted for the LTO-cycle). Following the ICAO, and other work in this field, reveals though that such regulations most probably will be established in a not too far future. A qualified estimate of a conceivable measure that has been mentioned in this context is a maximum allowed *15g NOx per kg fuel* (i.e. an emission index for NOx, i.e. EINOx < 15g/kg). This value has been used as a benchmark in the studies performed. Initial computations on the baseline M6T concept show wEINOx[2] values of the order of 250 g/kg, i.e. far above the 15g/kg benchmark. This high NOx production is mainly due the high temperature regime in which the engine is operating. A way to reduce this NOx production could be a staged combustion of RQL-type, though it is still doubtful if, and how, acceptable levels could be achieved. This doubt is partly due to questions regarding time scales and residential times for combustion products. Simulations of a RQL ("Rich-Quench-Lean") combustion, given the M6T baseline input conditions, indicate that NOx levels can not be significantly reduced by applying this principle alone. Probably it would be needed to go down significantly in combustor inlet temperature to achieve EINOx values an order of magnitude lower even with this technology. The most promising, hydrogen based concept, considered is a Lean-Direct-Injection (LDI), which indicated NOx levels approaching "acceptable" given the baseline combustor inlet conditions. The lower fuel rate in this case naturally gives a weaker thrust, resulting into a need for more or larger engines, and would thereby be linked with a re-design of the vehicle. This lower LDI fuel-air-ratio (equivalence ratio around 0.25) is also found to give a close to optimum engine over-all-efficiency, given the M6T baseline inlet combustor conditions.

While the RQL and LDI methodologies are already existing combustion technologies for turbo-fans, another more drastic methodology is a proposed separation of intake air into oxygen and nitrogen. The original application for this technology, so far only studied theoretically within the rocket/space community, was to fuel up oxygen in re-launcheable spacecrafts, but herein seen as a possible way to avoid nitrogen/oxygen mixtures reaching critical NOx production temperatures. Beside the system level integration matters, which are not studied herein, the approach indicates severe difficulties already in reaching acceptable NOx levels even at this principal stage.

[2] wEINOx is defined, and used, in this work in order to enable direct comparisons with aircraft engines using hydrogen instead of kerosene as fuel. In wEINOx, the "w" denotes "weighted EINOx", which means that the higher energy value of hydrogen, compared with kerosene, has been included by a factor of around 1/3 which is more relevant for direct EINOx comparisons with aircraft fuelled with kerosene.

Though, general considerations, supported by chemical equilibrium computations, indicate that the M3T concept most likely could come close to acceptable NOx levels. Both the M3T and the M6T are supposed to cruise around the altitude of maximum ozone concentrations (circa 25 km), where the NOx tend to reduce O_3 concentrations, which makes the ozone layer issue more critical than for subsonic aircraft cruising at the half of this distance from ground

1.3 Specific highlights

Due to the relatively low engine temperature approach, the M3T constitutes a promising general design regarding low NOx.

The wide flammability range of hydrogen, in combination with the short combustion times (i.e. a possibility for short combustion chambers), enables, at least in theory, possibilities to reach rather low NOx values for a concept of the ATLLAS M6T type. This is assuming that a sufficiently low fuel-to-air ratio could be applied[3].

1.4 Forms of integration within the ATLLAS Project

The work is linked with conceptual studies within WP2, for the M6T as well as for the M3T concept. Baseline engine input, for emission studies in WP4.6, was determined within WP2.

1.5 Note

NOx estimates shown in a well known text book, "Hypersonic Airbreathing" AIAA education series [1], is misleading. This ambiguity was not cleared out until a direct contact with one of the authors was established. It was then concluded that the NOx levels given, in the otherwise very well written book, were based on a mistake, and by this given far too low therein.

[3] In order to achieve these "acceptable" NOx levels it would be needed to reduce the equivalence ratio from 0.42, as for the ATLLAS baseline M6T at cruise, to around 0.25. Implying reduced thrust and thereby further re-designs.

2 NOx and the atmosphere

2.1 Climate Change

The last decades the knowledge and concern about global warming, the "greenhouse effect", has evolved considerably. All combustion processes, such as those in aeroengines, involve chemical reactions which add combustion products that may contribute to this effect, or in other ways negatively influence the atmosphere and thereby life on earth.

The main emissions from aircraft are CO_2, H_2O ("greenhouse gases"), NOx (i.e. nitric oxide – NO and nitrogen dioxide - NO_2), SOx (sulphur oxides), and soot. These gases and particles alter the concentration of atmospheric greenhouse gases, including also ozone (O_3) and methane (CH_4); trigger formation of condensation trails (contrails); and may increase cirrus cloudiness - all of which contribute to climate change.

An increase in atmospheric CO_2 and H_2O (gas phase) concentrations + contrails (from H_2O both in the exhaust and surrounding air, condensation triggered by exhaust) contribute to changes in the net radiative forcing, and are considered to give the strongest effect on earth surface temperature rise from aviation (year 2000 data) [2], [3]. In this context it could be mentioned that aviation is accounted for about 2% of all global CO_2 emissions according to the 4th IPCC assessment report [4].

The net radiative forcing effect from aircraft NOx is more complicated to estimate[4], and thereby also linked with a bigger uncertainty. First: it is indirectly involved in ozone production in the troposphere[5] (via the oxidation of CO). Secondly: NOx reduces the atmospheric CH_4 concentration. Third: in the stratosphere[6] NOx influences the destruction rate of ozone directly as a catalyst and indirectly by reactions with halogen free radicals. (see more about ozone and NOx in the next paragraphs). Both CH_4 and O_3 are strong greenhouse gases, meaning that the two first mechanisms are partly cancelling out each other, regarding the net radiative forcing effect. See Fig. 1 below. The scenarios behind the Fig. 1 graph are based on subsonic flight in the upper troposphere and lowermost stratosphere.

[4] This holds also for the amounts emitted from aircraft. While CO_2 and H_2O are created in direct proportion to type and amount of fuel burnt, the NOx quantity produced is related to the specifics of the combustion process.

[5] *Troposphere:* the first layer of the atmosphere contains 75% of the atmosphere mass and 99% of the water vapour, stretching from ground up to 5 - 20 km, depending on latitude and season, typically to ca 10 km. Temperature decreases with altitude.

[6] *Stratosphere:* the second layer of the atmosphere, temperature increasing with altitude. From about 10 to 50 km altitude at moderate latitudes, starting at ca 8km around the poles and could start as high as at 20 km in tropical regions (the level in between the troposphere and stratosphere, where the temperature change with altitude changes sign, is called the *tropopause*)

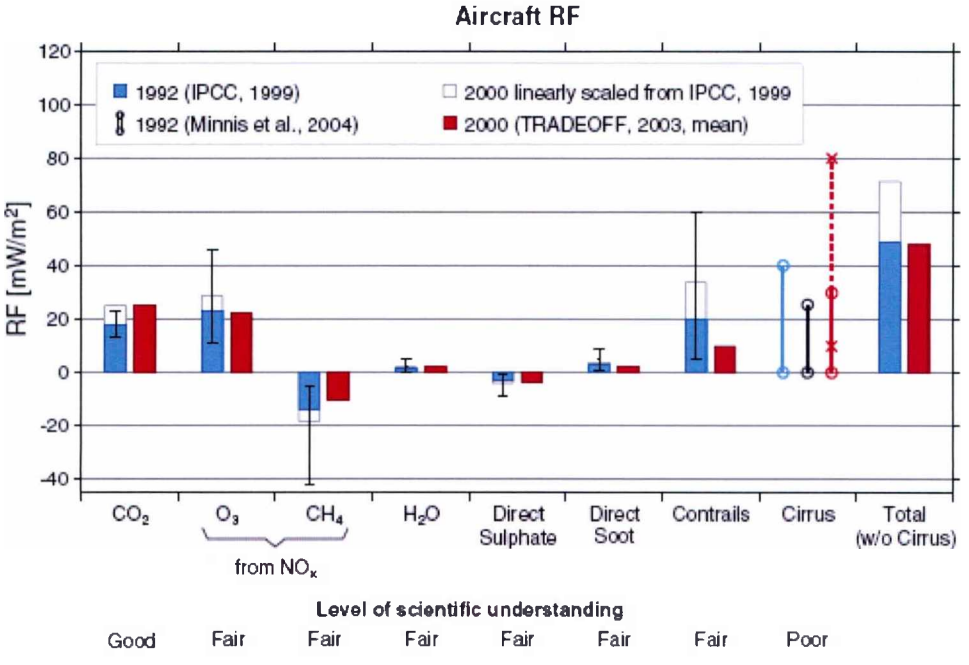

Fig. 1 **Radiative Forcing, RF [mW/m^2] from aviation for 1992 and 2000 based on IPCC (1999) and TRADEOFF results [3].**

Explanations to Fig. 1:
The vertical bars denote the 2/3 confidence intervals of the IPCC (1999) value. The lines with the circles at the end display different estimates for the possible range of RF from aviation induced cirrus clouds. In addition the dashed line (with crosses at the end) denotes an estimate of the range for RF from aviation induced cirrus. The total does not include the contribution from cirrus clouds.

NOx in the stratosphere is primarily produced from oxidation of N_2O (nitrous oxide or "laughing gas"), in turn originating mainly from agricultural soil management. While N_2O is inert in the troposphere the primary NOx sources here are directly coming from fossil fuel combustion (largest source, whereof 95% is from emissions in the northern hemisphere), biomass burning, soil emissions, lightning, transport from the stratosphere, ammonia (NH_3) oxidation and aircraft exhaust. This generation, plus transport mechanisms, governs the amount of NOx found at different altitudes in the atmosphere. The concentrations are found to be about 100 pptv at the tropopause and increasing to as much as 3000 pptv at an altitude of 20 km (N_2O has been found to increase with about 0.5-0.8 ppbv/year) [2].

The influence on the radiative forcing from different air traffic scenarios for the time up to year 2050 was estimated in [2] and is summarised in Fig. 2. To notice here are: 1) that the total radiative forcing is mainly a function of fuel consumption (e.g. emitted CO_2) 2) All of these scenarios assume that technological improvements leading to reduced emissions will continue in the future and an ideal air traffic management is achieved by 2050. 3) If these improvements do not materialize, then fuel use and emissions will be higher. 4) For the scenario with a supersonic fleet this fleet is considered to be of 1000 aircraft (compared with 12000 civil aircraft for the year of 1997) cruising at 19 km altitude with very low NOx levels assumed, 5g NOx/kg fuel. 5) radiative

forcing due to aviation (without forcing from additional cirrus) was likely to be within the range from 0.01 to 0.1 W/m^2 in 1992, with the largest uncertainties coming from contrails and methane. Hence the total radiative forcing may be about two times larger or five times smaller than the best estimate. For any scenario at 2050, the uncertainty range of radiative forcing is slightly larger than for 1992, but the largest variations of projected radiative forcing come from the range of scenarios. When considering the green-house effect, it could be mentioned that, according to ref. [5], recent CO_2 emissions are in level with or exceeds the "worst case" – IPCC [7] scenario studied.

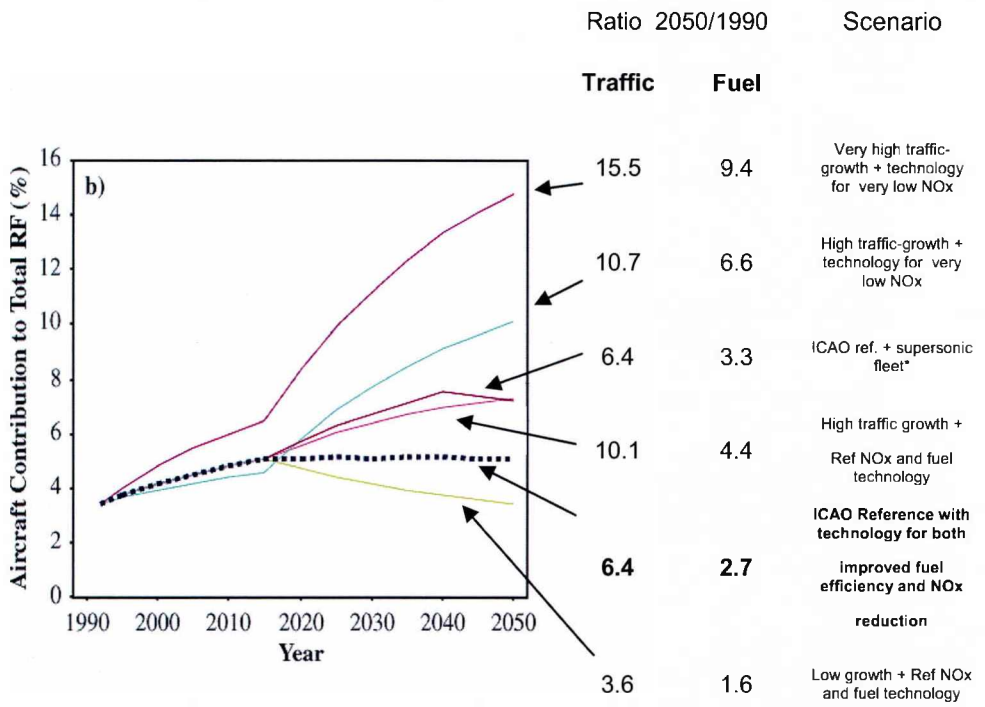

Fig. 2 Estimates of the globally and annually averaged total radiative forcing (without cirrus clouds) associated with aviation emissions under each of six scenarios for the growth and technology of aviation over the time period 1990 to 2050. from [2] with condensed information about the different scenarios fitted in to the right panel.

[7] the UN Intergovernmental Panel on Climate Change

2.2 The ozone layer

The concept "ozone layer" refers to the high concentration of ozone in the stratosphere, where about 90% of all ozone is residing. The thickness of ozone layer – meaning the total amount of O_3 in a column of the atmosphere overhead (if brought down to sea level, this "layer" would typically be a few mm's thick) – varies strongly over time and latitude. The ozone is created by UV-radiation from the sun mainly in the tropical middle stratosphere and predominantly brought to the extratropical regions (latitudes between 30° and 60°) of the stratosphere in the winter hemisphere, by a pumping action of wave induced forces, creating maximum ozone concentrations in the lower polar stratosphere appearing in (polar)spring. This dominating transport mechanism is called the Brewer-Dobson circulation.

Different transport modes correspond to different time scales, ranging from days to years. Stratospheric ozone is not only transported but also destroyed via photochemical reactions over the whole stratosphere. Ozone formation and destruction rates increase with height and change with latitude in the stratosphere. Consequently, ozone "lifetime" decreases with altitude from about a year in the lower stratosphere to minutes in the upper stratosphere.

In summary, stratospheric ozone distributions are determined mainly by atmospheric motions in the night time polar regions, by a mixture of transport and photochemistry in the lower and middle stratosphere, and by photochemistry in the upper stratosphere [2].

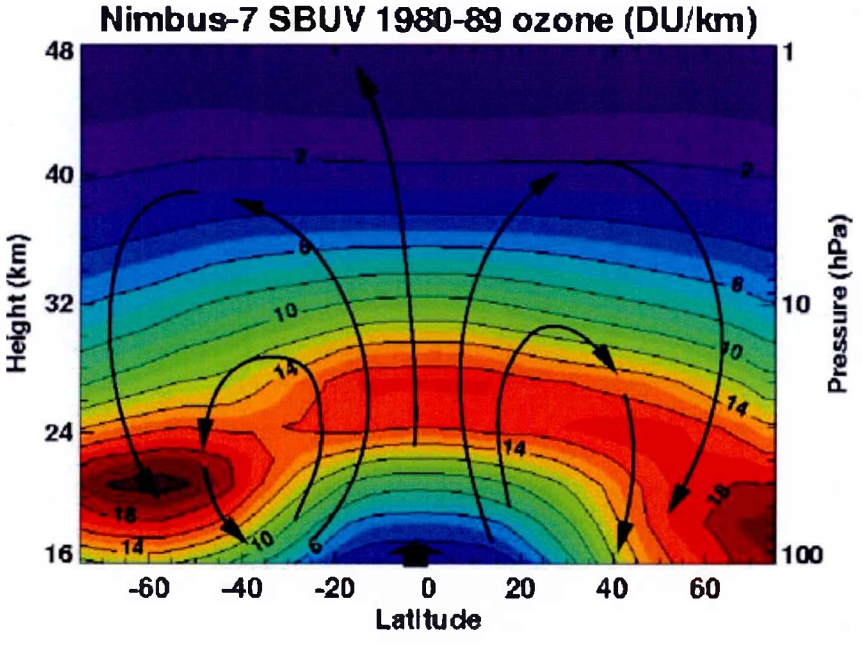

Fig. 3 **Meridional cross-section mean of the ozone distribution in the stratosphere as measured from the Nimbus-7 satellite 1980-89 with the Brewer-Dobson circulation shown. Concentration in DU/km (NASA).**
(DU=Dobson Unit, refers to a layer of ozone that would be 10 µm at sea level conditions).

From the unit DU a baseline value of 220 DU has been chosen as the starting point for the definition of an ozone hole. This since total ozone values of less than 220 Dobson Units were not found in the historic observations over Antarctica prior to 1979. Due to the ban on chlorofluorocarbons ("freons" or CFC's) in the late 70-ies, followed by a complete worldwide production stop in 1996, the ozone layer is expected to recover. According to several sources the Antarctic ozone hole is estimated to be healed during the second half of this century, this is assuming that no big changes in emission patterns or the understanding of atmospheric science occurs meanwhile. Though, this estimated moment of recovery has been pushed forward several times since the CFC's regulation entered into force, recent satellite measurements show a promising positive or at least leveling out trend [6]. From 6 different satellite measurements of the upper stratosphere (35-45km), between lat. 30° and 60° North, an ozone reduction of around 7% per decade (7.2 ± 0.9%) was found between 1979 and 1997. From 1997 to 2008 instead an increase of about 1% (1.4 ± 2.3%) could be found, the uncertainty to be noted.

Recent estimates of future ozone threats points out nitrous oxide (N_2O, or "laughing gas"), through conversion to NOx in the stratosphere, as the most alarming ODS (ODS =Ozone Depleting Substance, ODP=Ozone Depleting Potential), see Fig. 4. And suggest a limiting of N_2O in order to cure the ozone layer, which would also have positive effects regarding the global warming [7].

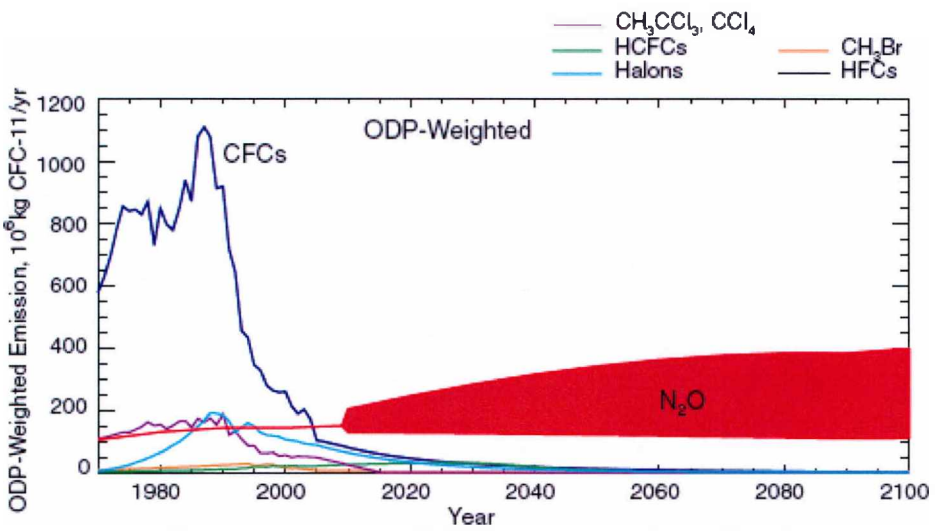

Fig. 4 Historical and projected ODP-weighted emissions of the most important ODS's [7].

The stratospheric and upper tropospheric ozone is vitally important to life because it absorbs the biologically harmful ultraviolet radiation from the sun. Based on wavelength there are three different types of ultraviolet (UV) radiation. These are referred to as UV-a (400-315 nm), UV-b (315-280 nm), and UV-c (280-100 nm). UV-c could be extremely harmful to humans and other life on earth, while UV-b, causing sunburn, is harmful in large doses. Fig. 5 gives a schematic view of how far into the atmosphere the different

types of UV-radiation reaches due to the stratospheric ozone. For example the UV-b radiation intensity at the Earths surface would be $350 \cdot 10^6$ times bigger without any atmosphere [8].

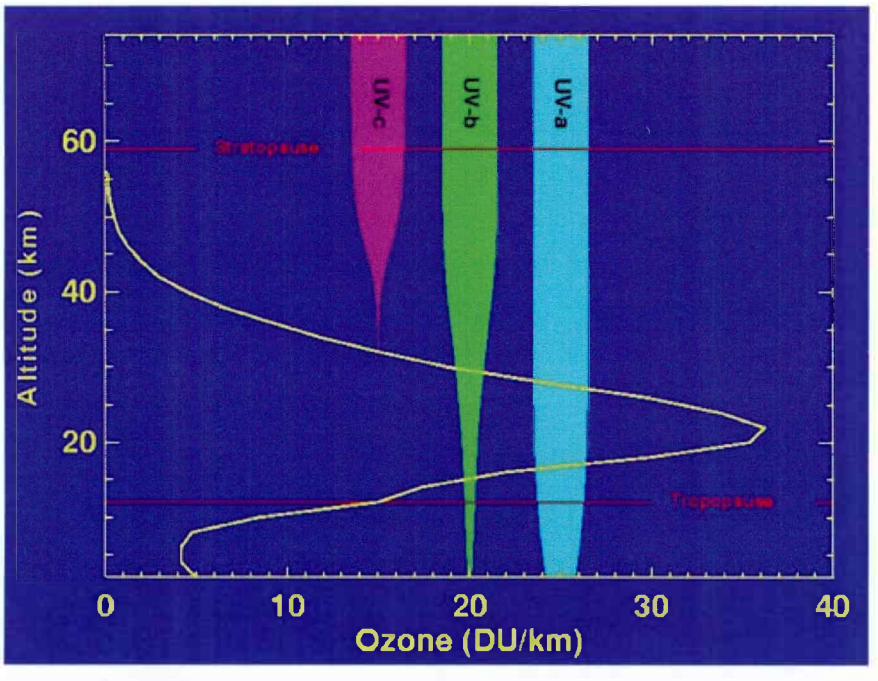

Fig. 5 **Mid-latitude ozone vertical profile and altitude of UV-a,-b, and -c penetration (NASA).**

2.3 NOx and the ozone layer

Though there is no evidence found for any appreciable change in the stratospheric NOx concentrations (IPCC 1998) [2] from aircraft exhaust, this and the related risk for ozone destruction, has in the past been one of the obstacles for previous SST projects. Seen in a global perspective, and starting out from the current understanding of atmospheric science, the influence on net radiative forcing from exhaust emissions by a limited SST fleet could most probable be regarded as marginal, but of course still of strong concern due to the efforts of reducing the "global warming". Most likely also for future SST projects the task of ozone layer depletion will be the most important obstacle to overcome regarding exhaust emissions. Assuming a fuel and combustion that is "clean" in terms of soot, particulates and aerosols, NOx emissions has in this study been viewed as the emission matter of strongest concern with regard to the ozone layer. Some circumstances behind this approach, as well as behind the risk of NOx causing stratospheric ozone depletion, are:

1) a SST of the studied type will spend most of the time well above the tropopause in the stratosphere (typically at an altitude of 27 km), unlike a subsonic fleet which is flying in the upper troposphere or lowermost stratosphere (9-13 km).

2) the longer residence time for exhaust gases in the stratosphere. (The average residence time for aircraft exhaust gases in the lowermost stratosphere, i.e. altitude of subsonic aircraft of today, is about 6 months, but for emissions between 25 and 30 km average residence times goes up to about 5 years) [9].

3) The transport processes at these altitudes (above 20 km) and stratospheric-tropospheric exchange, are governed by global-scale vertical circulation which remains considerable uncertain ([9], 1998). This uncertainty is partly because of the limited amount of measurement data gathered from this region of the atmosphere.

4) At the high total temperature conditions related to supersonic flight, especially for RAM-jet engines, basic chemistry predict very high NOx emissions.

In the stratosphere, NOx both catalytically destroys ozone via:

O_3 + sunlight $\rightarrow$ O + O_2 (ozone destruction through photolysis)
O + $NO_2 \rightarrow$ NO + O_2
NO + $O_3 \rightarrow$ NO_2 + O_2

Net: 2 $O_3 \rightarrow$ 3 O_2

and also acts to interfere with the destruction of ozone by reactions of HOx and halogens. As a result of these coupling reactions, involving NOx, HOx and halogens, changes in the concentration of NOx can lead to increased or decreased rates of stratospheric ozone destruction. In regions where NOx is high, ozone destruction increases. On the other hand, the opposite occurs in the lower stratosphere because the increased NOx decreases the loss of ozone by hydrogen and halogen radicals. Thus, as with the production rate of ozone in the troposphere, the response of ozone destruction with changes in NOx is highly nonlinear. The loss during the month of March as a result of catalysis by each family, i.e NOx, HOx and halogens, is illustrated in Fig. 6, left panel. For this latitude and season, the loss is dominated by halogen and hydrogen oxides below 20 km, whereas above 25 km, nitrogen oxides are most important.

When NOx is low - as it is in most of the lower during winter, fall, and spring - most of the ozone loss occurs through HO_x and halogen chemistry. Under these conditions, enhancements of NOx will decrease ozone destruction. On the other hand, at higher altitudes and during summer, NOx-catalyzed ozone loss (reactions above) can dominate the removal of lower stratospheric ozone, so enhancements in NOx will speed up ozone loss. These effects have been demonstrated by direct measurements of free radicals in the stratosphere. The right panel in Fig. 6 shows the effect of a uniform 20% increase in the concentration of NO.

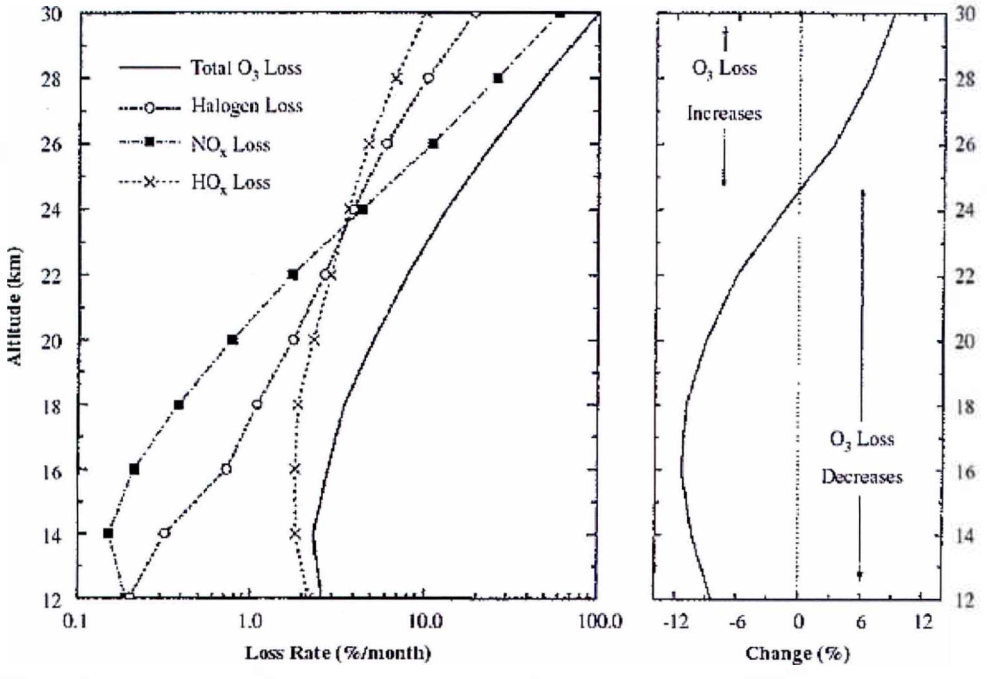

Fig. 6 Calculation of the rate of ozone loss in the lower stratosphere for springtime mid-latitude conditions during March [2].

The change in ozone loss rates illustrated in Fig. 6, panel 2, does not translate directly into a change in ozone. For example, for a uniform 20% increase in NOx, enhanced loss rates at high altitudes will reduce the transport of ozone to the lower stratosphere. As a result, ozone concentrations in the lower stratosphere can decrease even when the local ozone loss rate slows. Thus, the change in the ozone column with added NOx is very sensitive to the altitude distribution of the perturbation. The subsonic aircraft fleet adds NOx only to the lowermost stratosphere (< 13 km), where large-scale dynamics tend to prevent advection to higher altitude. As a result, injection of NOx by the present subsonic fleet is thought to increase ozone in the lower stratosphere [2] , while a supersonic fleet at altitudes around 25 km would decrease the ozone due to NOx emissions. Its worth noting that this pattern is found, though "natural" NOx concentrations, as well as O_3 concentrations, at these altitudes are much higher than in the upper troposphere.

More recent predictions of the risk for a ozone layer depletion by a future fleet of supersonic aircraft are given in [10] and [11]. In ref. [10], a NASA study supported by Boeing, one compares different supersonic fleet scenarios with a subsonic ditto regarding ozone layer impact based on 2-D chemical transport models of the global atmosphere. This study shows a stronger ozone reduction impact than the IPCC (1999) assessment [2], given NOx emissions of the same size. Series of parametric analyzes that examined a range of total fuel burns (33 to 66 million kg per day), EINOx values (5, 10 and 20 g/kg/fuel) and cruise altitudes (13 - 15, 15 - 17, 17 - 19, and 19 - 21 km) were undertaken. The study concentrates on a relative comparison of ozone columns for a fleet of 500 supersonic aircraft that replaces a part of a subsonic 2020 scenario fleet. Results represent steady state model simulations where the model is run for 10

years. The main findings, according to the applied model, were: most combinations showed an ozone layer depletion compared with the subsonic scenario with the strongest reduction resulting for the "maximum" case in terms of fuel burn (66.000 tons a day), EINOx (20 g/kg fuel) and altitude (19-21 km). I.e., an expected increased depletion with altitude and amount of NOx. For the northern hemisphere this scenario showed a total ozone column reduction, compared with the subsonic scenario, of 0.86%, with a maximum local reduction of 2.2%. The distribution of this prediction, over the year and latitude is shown in Fig. 7.

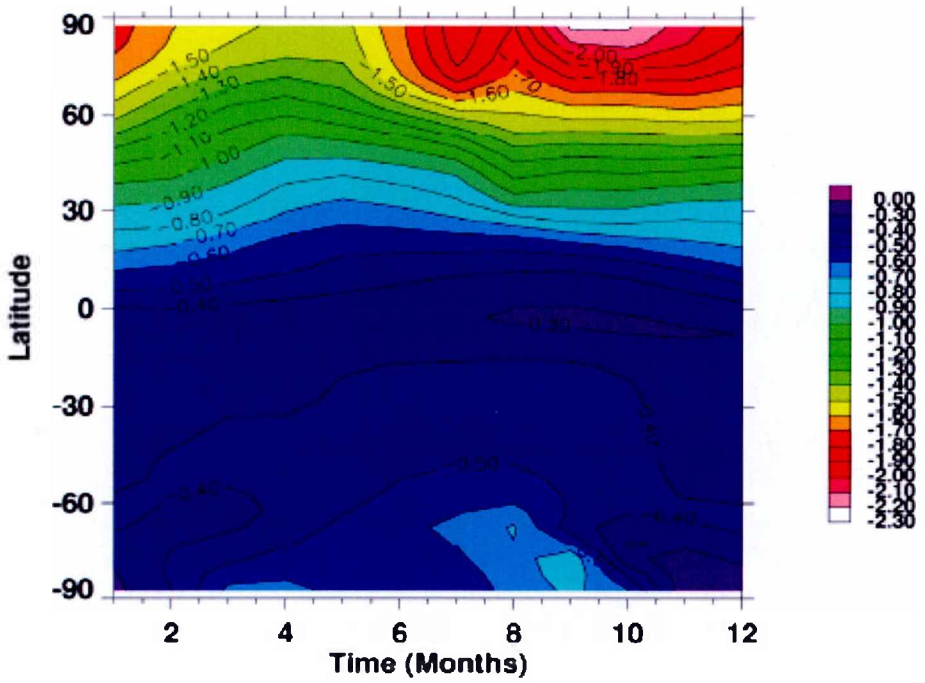

Fig. 7 Total ozone column change in % for the "worst" supersonic fleet scenario compared with an exclusively subsonic scenario [10].

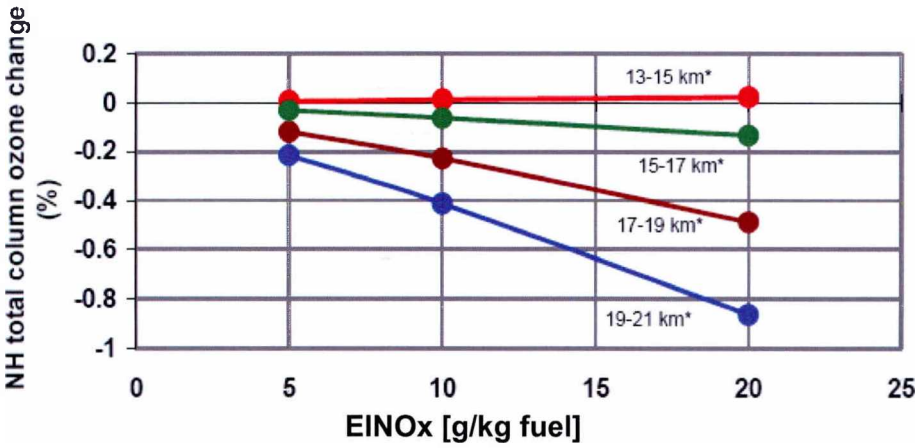

Fig. 8 **Northern Hemisphere total ozone column change for the 66 kton/day fuel scenario [10] fig. from NASA, (*altitude bands).**

Fig. 8 shows the variation of ozone column change for the maximum fuel burn scenarios with altitude and EINOx. The modelled increased destruction with EINOx and altitude is very clear here. One should here keep in mind that the results are based on a rather big fleet of 500 aircraft. From results in [10] one can see that the predicted ozone column destruction roughly varies linearly with the amount of emitted NOx, and might be scaled by this rule of thumb as a first estimate.

2.4 Other NOx effects

Beside the risk of ozone layer depletion in the stratosphere, NOx emissions have negative effects also closer to ground. As in the upper troposphere NOx participates in ozone production which causes health problems, such as injures on lung tissue through chemical reaction, damages plants and crop and generates smog. This is the reason behind why NOx emissions are strongly regulated regarding energy production from fossil fuels, ground vehicles and aircraft [12], [13]. Up to date only standards for the LTO-cycle for aeroengines exist (based on engine certification tests on ground). Though, ongoing work is directed towards potential coming standards covering higher altitude/cruise flight.

2.5 NOx generation

NOx could be formed through three major sources in combustion[14],[15] :

1) Thermal NOx (Zeldovich mechanism) - oxidation of atmospheric nitrogen.

This mechanism is the dominating source of NOx for aeroengine combustion for clean fuels (not containing nitrogen compounds). The process peaks in the flame front were the temperature peaks but goes on as long as the temperatures are kept "high". The principal reactions comprising thermal NOx formation are:

$$O + N_2 \rightarrow NO + N$$

$$N + O_2 \rightarrow NO + O$$

$$N + OH \rightarrow NO + H$$

The thermal NOx production is exponentially dependent on temperature and linearly dependent upon time. This is the basic mechanism behind the NOx generation in the chemical kinetics studies in this work.

2) Prompt NOx (Fenimor mechanism) – reactions involving hydrocarbons fragments and atmospheric nitrogen are believed a source of nitrogen radicals, which subsequently oxidises to form NO:

$$CH^* + N_2 \rightarrow HCN + N^*$$

$$CH_2 + N_2 \rightarrow HCN + NH^*$$

These actions take place in the fuel (hydrocarbones) rich zone of the combustor.

3) Fuel NOx – occur when fuel bound nitrogen is oxidised. Not an issue within ATLLAS, or for aircraft engines in general (but mainly for coal derived fossil fuels).

With hydrogen fuel only the first mechanism, 'thermal NOx', will contribute. At the high combustor inlet temperatures at cruise the first mechanism will dominate also for hydrocarbon fuels.

2.6 Future NOx restrictions

The International Civil Aircraft Organisation, ICAO has, through its sub-committee CAEP (Committee on Aviation Environmental Protection), established current regulation limits as well as future goals for aeroengine NOx emissions. The most recent standards, CAEP 6, took effect on January 1, 2008 for newly certified engines. Outgoing from these engine NOx certification requirements, future goals imply approximately a recommended 25% sharpening up to 2016 and 60% to year 2026 [16].

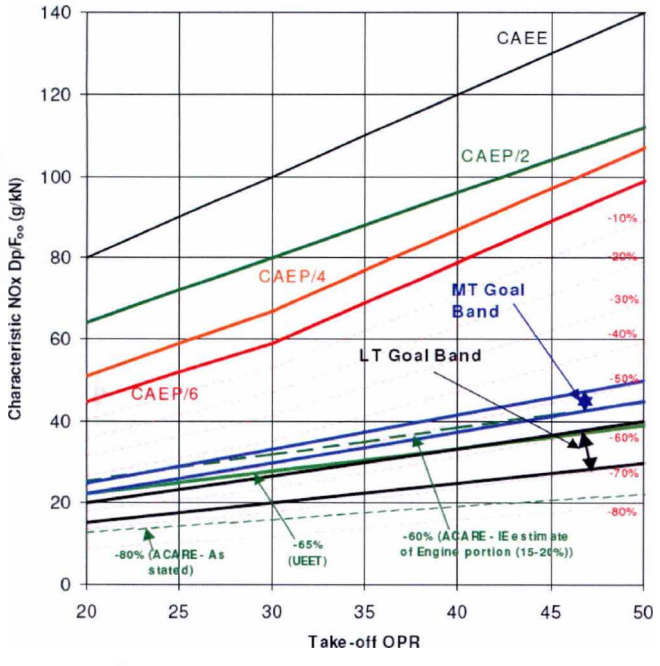

Fig. 9 CAEP certification limits with industry and research programme targets [17].

The limitations are stated in Dp/Foo which means "in grams of NOx per kN of maximum thrust during a reference LTO-cycle, below 3000 feet, as a function of OPR" (OPR = Overall Pressure Ratio). Another applied measure for NOx emissions is EINOx, (EI=emission index), given in grams NOx/kg fuel. Dp/Foo and EINOx values are related but not directly convertible. Both these measures (for the LTO-cycle) can be found in the ICAO Engine Emissions Databank (for civil turbofan engines) [18].

With supersonic flight in focus one should note:

1) ICAO standards on NOx limitations have *not yet taken into account cruise NOx emissions*. Such recommendations will most possible be established in the future.

2) *No up-to-date limitations exist for supersonic flight* even for local air quality (the ones that have been stated in the past for the LTO-cycle dates back to the Concorde). Most likely future rules for supersonic aircraft will agree with regulations for subsonic aircraft [19].

Similar to the fundamentally different noise situation encountered for supersonic flight, vs. subsonic, the matter with NOx emissions becomes much more critical for supersonic (turbo jet) engines. As outlined above, the main NOx contribution -"thermal NOx" - is exponentially proportional to the temperature. Already for turbojets this means that we have a different situation at supersonic flight as shown in

Fig. 10 below (from [19]):

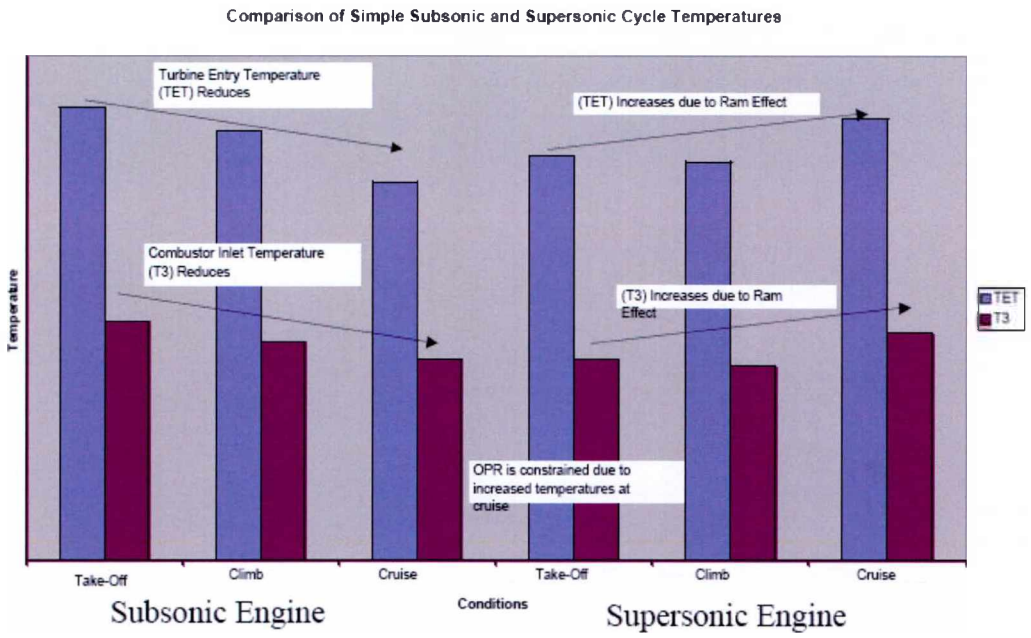

Fig. 10 Combustor temperature conditions for sub- and supersonic engines (T3=Combustor inlet temp., TET = Turbine Entry Temp.) [19].

We see here, in contrary to subsonic engines, that both T3 and TET tend to be higher at cruise than at take-off, with an expected higher NOx emission at cruise. In the cruise RAM-jet phase, for a combined cycle engine such as in the ATLLAS concepts, this situation will be even more clearly expressed as indicated below (M6-concept).

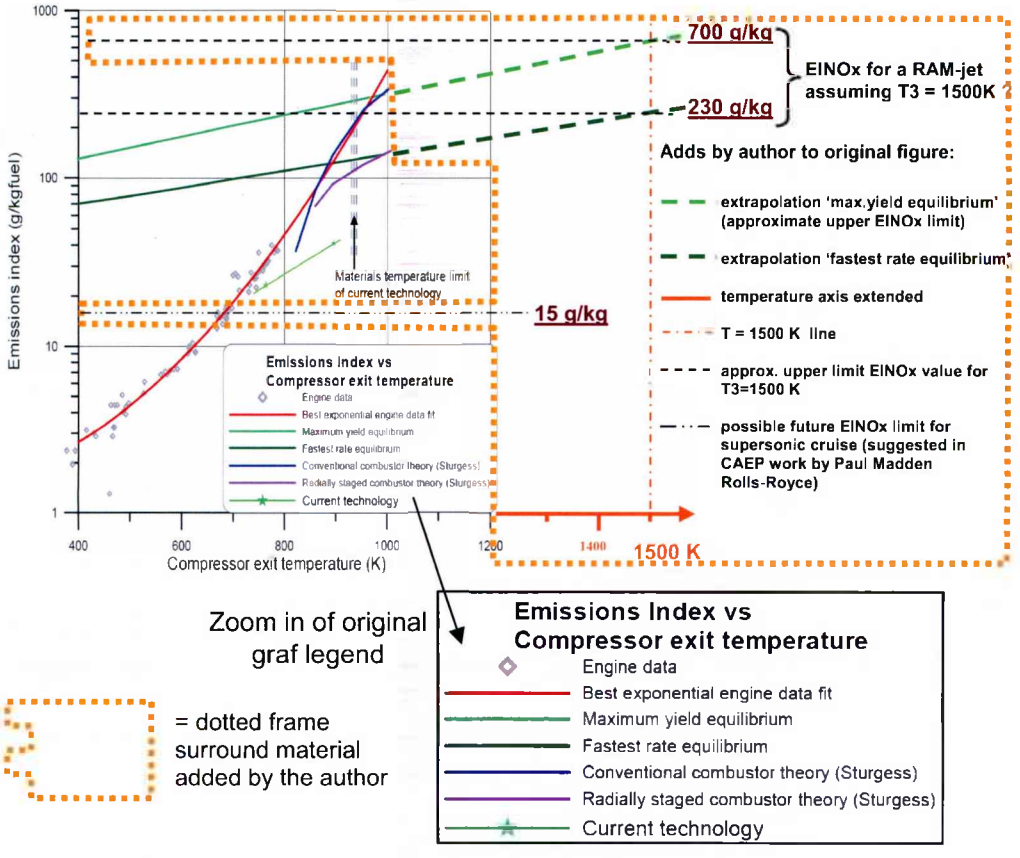

Fig. 11 NOx as a function of combustor air entry temperature. From [16] with example RAM-jet data and possible future regulation limit added by author (added info within orange dotted line region).

Fig. 11 shows (from [16]):

"NOx Emissions Index (EINOx) as a function of combustor air entry temperature (compressor exit temperature). The NOx production is also a function of pressure that is taken account in the data since the pressure is a function of the temperature (any effects of variations in compressor efficiency will be lost in the scatter). Two theoretical NOx characteristics are shown [from the EU project Cypress]. The line 'maximum yield equilibrium' shows the NOx that could be generated by the most effective air/fuel ratio given 'infinite' reaction time. However 'infinite' in this context can be measured in unit milliseconds. The line 'fastest rate equilibrium' shows the NOx that could be produced at a fuel/air ratio that generates NOx at the fastest possible rate. These two equilibrium lines together with all the intermediate possible levels are produced at similar air fuel ratios and temperatures close to the maximum flame temperature that will be present in the primary zones of all 'conventional' and RQL[8] combustors."

Taking the original figure and extrapolate EINOx values for 'maximum yield equilibrium' for a RAM-jet combustor inlet temperature (T3) of 1500 K[9], as

[8] RQL = Rich-burn/Quick-mix/Lean-burn (se § 2.4 below)

[9] The combustor inlet temperature of 1500 K can be taken as a typical value for a RAM-jet driven aircraft flying at around Mach 6 in the lower stratosphere.

done in Fig. 11, gives a rough estimate of an EINOx value of 600-700 g/kg fuel, i.e. far above newer turbofans and current technology for more moderate temperatures shown in Fig. 11. These considerations indicate the huge step required for RAM-jet NOx reduction methodologies in order to reach emission levels comparable with those of subsonic engines of today. This need is further emphasized in work carried out by CAEP and summarised in the presentation in reference [19] where a possible EINOx target for future supersonic cruise is thought to be 15 g/kg (RAM-jets are not considered within ref.[19]). Even for turbojet engines this target implies a significant improvement compared with available combustion technology of today. An other aspect that could strengthen the EINOx requirements even more on commercial supersonic aircraft, is that an environmental impact measure, applied for comparison with subsonic flight or other kinds of transportation, could be of the type "emissions per passenger and distance".

For a direct comparison of NOx emissions from a hydrogen fueled aircraft, with one using conventional (kerosene) or other hydrocarbon fuel, one should take into account the higher heating value of H_2, i.e. the higher energy content in H_2. This might be done by a factor $h_{kerosene}/h_{H2}$, of the respective heating values ("lower" heating values, h_{H2}= 121 MJ/kg, $h_{kerosene}$= 43 MJ/kg) i.e. by a factor of around 1/3. Other possible fuels have heating values about the same as kerosene (methane = 55.5 MJ/kg, $h_{kerosene}/h_{CH4}$ = 0.86). Let us assume that the EINOx data given for T3 = 1500 K in

Fig. 11 above, roughly 600-700 g/kg fuel, was taken for H_2 fuel. Then these values could be reduced to around 200-250 g/kg for a direct EINOx comparison. (If emission index values are to be used for a trajectory computation for total emission over a part or over the complete flight track based on fuel consumption, off course the unweighted EINOx values should be used. On the other hand, related lower emissions for hydrogen would be reflected due to the relatively higher heating value/lower fuel mass consumption.[10])

Just to give an idea of how the EINOx value may vary through a flight cycle for a conventional turbo fan, Fig. 12 from [21] is shown. The LTO data, with its four certification points, are shown for each engine type. The Floatwall combustor gives an 11% margin to the CAEP/2 standard while the newer Talon meats the CAEP/4 standard. This study is one in the works towards a possibly coming cruise NOx standard (the work argues for staying only to one standard, the current LTO, and that cruise NOx data could be retrieved from LTO data through correlation).

[10] The much smaller density of liquid hydrogen fuel (0.07kg/liter), compared with kerosene (0.8kg/liter), bring about the well known drawback of hydrogen storage volume. The given data tells us that in order to store the same amount of chemical energy, liquid hydrogen needs approximately 4 times the volume of kerosene. So, the gain won with a smaller take off weight, for the same mission and a similar vehicle, is partly lost through a smaller pay-load volume.

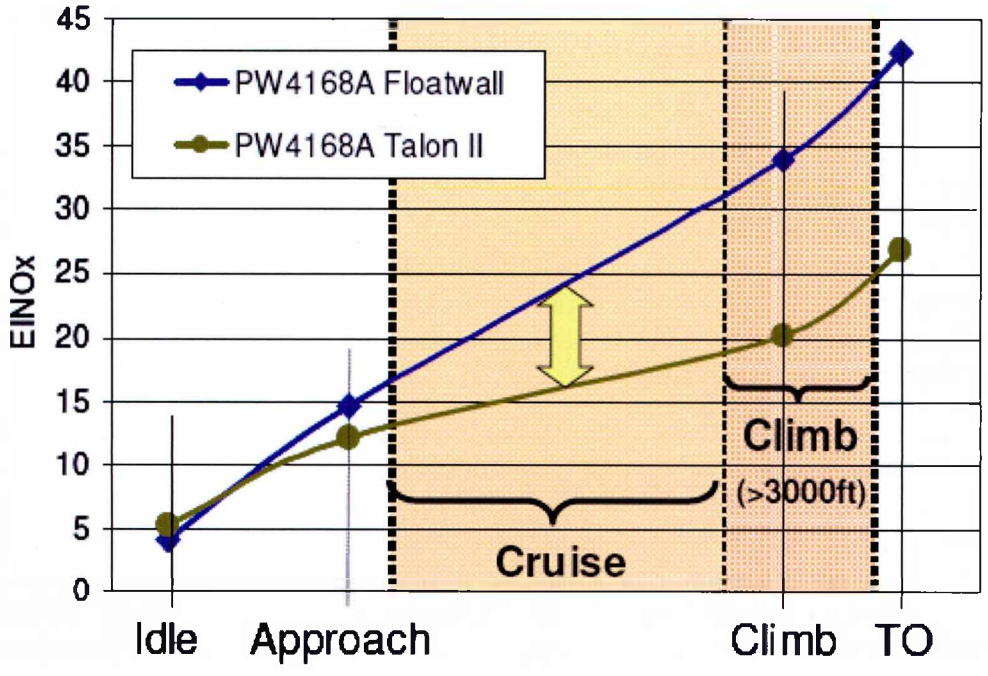

Fig. 12 **EINOx data in the four certification power setting points for a Pratt&Witney engine (PW4168A) with two different combustors (Talon II meet CAEP/4 standards) [21].**

3 NOx reduction methodologies

It was decided, already on the planning stage of the ATLLAS project, not to involve studies of the detailed mixing and combustion processes taking place in the combustion chamber. Accordingly the combustor is in WP4.6 more or less treated as a 'black box'. Though, since these matters are closely linked with the matter of NOx production, and have to taken into account to some extent, a literature survey on the fundamentals of combustion chamber technology, with focus on NOx generation was carried out.

This paragraph is a result of this literature study and outlines some combustion principles with a better low NOx potential than conventional combustors. The methodologies, found in the open literature, stretches from combustion systems already operational in aero-gasturbines, while others are regarded as promising from an early stage of research. The majority of these methods are developed for turbofans and unfortunately not directly applicable for RAM-jets. Further, only a few articles are touching the subject of RAM-jets and NOx emissions. Anyhow, together with the respective NOx reduction methodology, a coarse judgement of its possible applicability for RAM-jet combustion is made.

From the above described situation follows that the found material is also restricted regarding the type of fuel, as it basically concerns conventional kerosene fuel. The subject of hydrogen and CH_4 fuel combustion is though briefly addressed in the following.

3.1 Staged combustion

Fuel and/or air are injected into the combustion chamber at different stages along the main flow path. For modern gas turbines the injection is usually annular with secondary stages radial along combustion chamber walls. A staged combustor reduces NOx because the combustor has been optimised for high power NOx emissions by minimising the time spent at the peak production conditions (peak temperature at AFR[11] close to one).

In a first stage a fuel rich mix is ignited and burned. The resulting combustion products, containing some unburned fuel, are in a second step mixed and cooled with bypassed air. This fuel lean mix is then combusted. Staged fuel injection could probably be utilised to some extent, and beneficial, for RAM-jet NOx. (See principle in Fig. 13). Two concerns here are: The time spent (for combustion products) in the fuel rich and fuel lean zones and secondly the trade-off between engine overall efficiency and NOx levels. Given that the baseline cruise AFR for the ATLLAS M6 configuration at cruise (fuel=H_2) is already quite high due to other considerations, i.e. lean combustion, with an AFR= 5.7 (moles air/moles fuel) or an equivalence ratio of $\varnothing$=0.41 due to other considerations, not too much freedom is left to separate the fuel (H_2) injection into several steps.

[11] AFR=Air to Fuel Ratio

The lilac curve, 'Radially staged combustor', in Fig. 11 represents the staged methodology. As seen there the NOx generation for this type meets the 'fastest rate' chemistry curve (dark green) at high temperatures. Based on this fact, plus the added extrapolated dark green EINOx curve for higher temperatures, and assuming a combustor inlet temperature of 1500 K, an approximate minimum for a RAM-jet applying staged combustion technique is shown to be roughly 230 g/kg fuel.

3.2 RQL - Rich-burn/Quick-mix/Lean-burn (or Rich-Quench-Lean)

The RQL can be seen as one kind of staged combustion where an initial fuel rich combustion is followed by a fast injection of air giving a secondary zone of lean combustion. In this way the peak in NOx formation, as a function of Fuel-Air Ratio, is avoided (this peak is usually found close to stoichiometric values which gives the highest flame temperature). Or as described in ref. [21]:

(1) Fuel and small part of air react in rich stage. Mixture reconstituted to CO, H2 and heat. Very low NOx formation rate due to low temperature and low concentrations of oxygen

(2) Additional air rapidly added to produce lean mixture. Fast fuel-air mixing is critical to minimize NOx formation

(3) Lean mixture reacts at reduced flame temp.

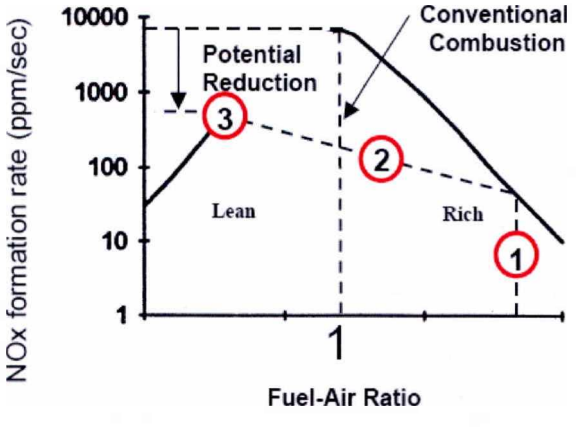

Fig. 13 NOx formation rate as a fcn of Fuel to Air Ratio with the three RQL steps added [21].

The RQL technique is studied as an alternative for a low NOx precooled turbo-ramjet fuelled with hydrogen in the LAPCAT II project [22]. The principle is pictured for a turbofan combustor in Fig. 14. This principle has to some extent been studied for the ATLLAS M6T concept in paragraph 5.9.1 (with non-satisfying NOx reduction results).

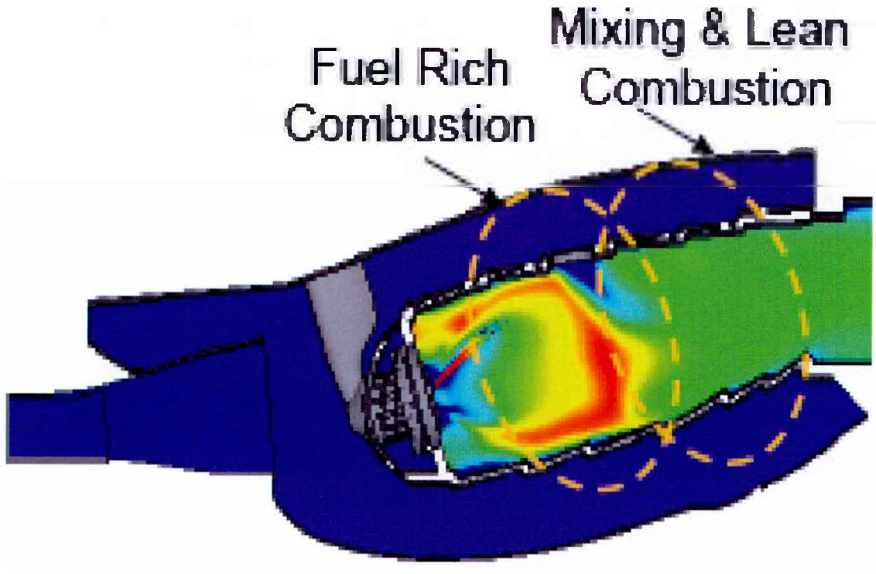

Fig. 14 RQL combustion principle (annular combustor) [23].

3.3 Lean Premixed Prevaporised (LPP)

The main idea Behind the LPP is that the fuel is vaporised before injection to the burner, achieved by a very high number of injectors and a set of pre-mixing chambers. Research has shown very strong NOx reductions but though the technique has been studied for some decades there are, according to [16], still difficulties linked with auto-ignition and flashback in premix ducts. Also problems due to resonance phenomena are reported. There is likely to be an impact of combustor length, due to a required set of pre-mixing chambers, leading to increased engine/aircraft weight. These and other issues remain largely unsolved problems even in methane burning land-based gas turbines where agile handling is not required. According to [16] LPP is unlikely to be a contending technology even in the long term.

The ref. [24] presentation, from academia, gives a slightly more optimistic vision for LPP combustion in the future.

In the HISAC project [25], where a small supersonic business jet was studied quite in detail, LPP combustion was considered as the alternative for low NOx for combined cycle turbo-jet engines.

None of the partly restricted combustion studies within ATLLAS is specifically accounting for the fuel vaporisation stage. By starting out from gaseous fuel, a "prevaporisation" could be seen as being included in all studied examples.

3.4 Lean burn direct injection (LDI)

Basically a derivate of the LPP, where a direct injection of the bulk of the fuel is sprayed with high velocity into a very turbulent flow in one lean zone (shortening engine length compared with LPP) where, in principle, stoichiometric peak flame temperatures are never achieved (see point 3 in Fig. 13). As for the LPP, even in this case a very large number of injectors is needed compared with a traditional injector/combustor design, which gives a more complicated engine both for construction and maintenance. Given the baseline combustor inlet conditions, this LDI-path was the only studied approach that showed possible NOx reduction success for the ATLLAS M6T concept.

3.5 Water injection

Water injection has from the 70-ies been extensively studied and applied as a means to reduce fuel consumption, increase thrust, maximum altitude, and/or flight speed of turbine engines. For industrial gas turbines the method has been in use also for NOx reduction for some time. More recently the technique has gained interest for NOx reduction also for aeroengines.

In [26] a water injection system for the low-pressure compressor (LPC) on turbofan engines[12] is studied with focus on climb-out NOx. The methodology is reported as promising, and could be summarised as: If the water misting rate was 2.2% water-to-air ratio (present industrial gas turbine rate) this could reduce NOx emissions some 47% from non-water misted engines.

In [16] the same study is interpreted as less optimistic, not regarding NOx reductions but due to related weight problems linked with tankage, pumping and pipework, plus additional logistics problems.

Also in [27] water injection at take off for turbofan has been studied as a method of NOx reduction. Herein, three different injection points were studied, LPC inlet, HPC (High Pressure Compressor) inlet and combustor, as shown in Fig. 15 and Fig. 16 below.

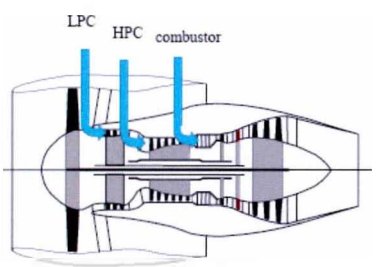

Fig. 15 Turbofan with examined water injection points (figure from ref. [27]).

[12] analyses were made on a high bypass turbofan engine of current technology baseline engine. Performance and the NOx emission index were similar to the General Electric GE90 and Pratt & Whitney PW4000 series engines

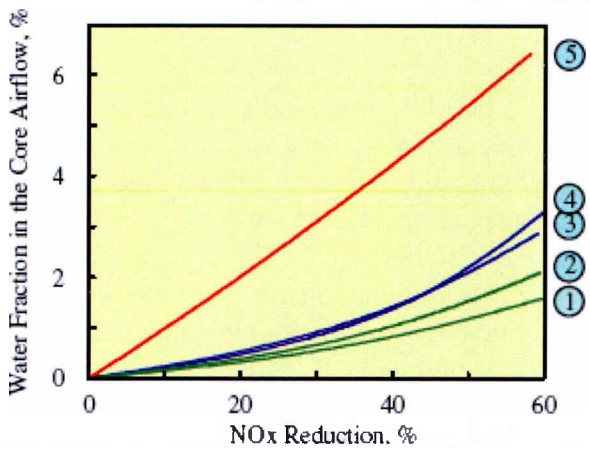

Fig. 16 Water fraction in the core air flow vs. NOx reduction (figure from [27])
When water is injected at the inlet of:
1) LPC, reduced cooling air bleed; 2) HPC, reduced cooling air bleed;
3) LPC, normal cooling air bleed; 4) HPC, normal cooling air bleed;
5) combustor.

In Fig. 16 LPC injection is found to be the most economical injection position in terms of required amount of water. Quite limited amounts of water are found to be sufficient to reduce NOx with 50%, 0.42% of total fuel storage when applied to takeoff and climb out. It is in the article argued that SST:s also could benefit from combustion water injection, not only because of NOx but also by mass augmented thrust gains in the transonic region and at cruise. The question of storage of water to be used during cruise is not raised in the article.

In contrary to the results found in reference [27], injecting water directly into the combustor was the preferred method for NOx reduction during takeoff according to [28], which goes more into the detail system requirements.

In summary, water injection is by some researchers found to be a promising way to reduce NOx in future turbofans. The methodology might as well be utilized in the LTO cycle for a combined cycle turbojet/RAM-jet ATTLAS engine (M3 and M6 configuration). No articles on this methodology, applied to RAM-jets, have been found in the literature review.

Only a very limited gain regarding NOx, by adding rather high amounts of H_2O in the combustion, was found though in an ATLLAS baseline example (see paragraph 5.9.4). However, if stronger gains of cruise NOx could possibly be found, only a small addition of water could be accepted due to weight concerns.

3.6 Catalytic Combustion

According to [16] it is hard to see that catalytic combustion could be an accessible path for low NOx aero gas turbines:

- It has not been possible to produce competitive catalytic combustion even for gas fuelled, land based gas turbines.
- Catalytic combustion is heavier and demands larger, longer combustion systems which could have a serious negative impact on engine/aircraft weight and fuel burn.
- Moreover, catalysts have a short lifetime (even more crucial within the high temperature range)

In summary it is stated: "This technology is unlikely to be viable even in the long term". For the RAM-jet one could add that it would be very difficult, without introducing tremendous pressure loss, to introduce a catalyst else then as a combustor liner, i.e. only a minor part of the NOx exhaust gases would be in contact with the catalyst and thereby reduced.

Selective Catalytic Reduction (SCR), a widely applied NOx reduction method for industrial gas turbines, uses a catalyst to react injected ammonia to chemically reduce NOx [12]. Since this methodology involves a catalyst, similar problems as mentioned above, holds.

With the SNCR (Selective Non Catalytic Reduction) technique, ammonia or urea is injected within the combustion chamber in a region where temperature is between ca 1250K and 1450K. This technology is based on temperature ionizing the ammonia or urea instead of using a catalyst. This temperature "window" – which is needed for the wanted reactions and reported differently by various authors - is important because outside of it either more ammonia "slips" through or more NOx is generated than is being chemically reduced [12]. Therefore it can be concluded that SNCR can not be applied for the ATLLAS M6T (already inlet temperature T3 around 1500 K) but there might be an opening for its use for the M3T configuration RAM-jet phase where temperatures are much lower. The extra weight, when carrying ammonia (also involving security aspects) or urea beside the fuel, has of course also to be considered in this case, especially for cruise conditions.

3.7 Trapped Vortex Combustion

Trapped Vortex Combustion (TVC) is the name of a technique where fuel and air are mixed in a limited space geometrically designed in the way that the flow generates a stable "trapped" vortex zone. According to [16] the TVC technique has the potential of increasing combustor performance including heat release rate operability, weight, costs and to some extent reduce NOx emissions compared with a traditional combustor with flameholders and swirl stabilized combustion. The principle is outlined in Fig. 17 and Fig. 18 below.

(Note: As mentioned previously the combustor design is out of scope within ATLLAS, and detailed combustor mixing processes not studied. The TVC is here only viewed as one possible technology that might find its application also in RAM-jet combustion.)

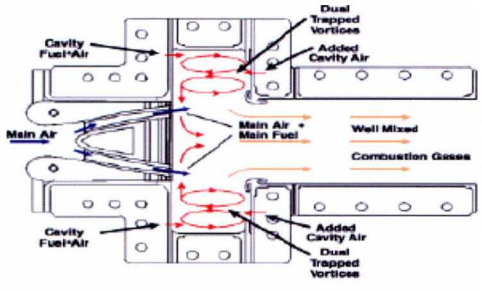

Fig. 17 Example TVC cross section (from [30]).

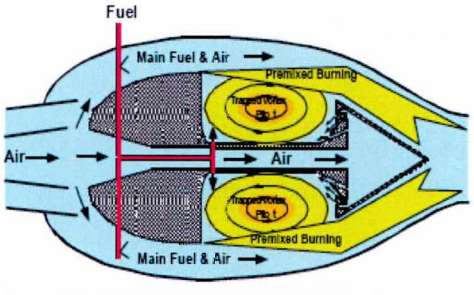

Fig. 18 TVC combustion layout example (from [29]).

3.8 Hydrogen fuel (fuel of ATLLAS M6T)

From [16] (for turbofans) :

- Both hydrogen and methane fuels could give significant NOx reductions because they have a wider flammable range,allowing operation at lower than peak flame temperature whilst maintaining at leaner air fuel ratios than would be possible with kerosene.
- Hydrogen and methane also have advantages of thermal stability and cooling capacity that could be beneficial in advanced engines.
- Both hydrogen and methane would increase emissions of water vapour at altitude that may or may not turn out to be significant to radiative forcing.

With the 100 K higher hydrogen flame temperature, compared with kerosene, follows that also the NOx production would be increased for stoichiometric combustion. However, hydrogen has a wider range of flammability and

therefore the entire operating range of the combustion zone may be shifted further into the lean region. Thus, to influence the NOx emissions, it is necessary to modify the fuel/air ratio in the primary combustion zone in a way that fuel lean combustion is realized at all load conditions without suffering a flame-out [31]. This situation is exemplified in Fig. 20.

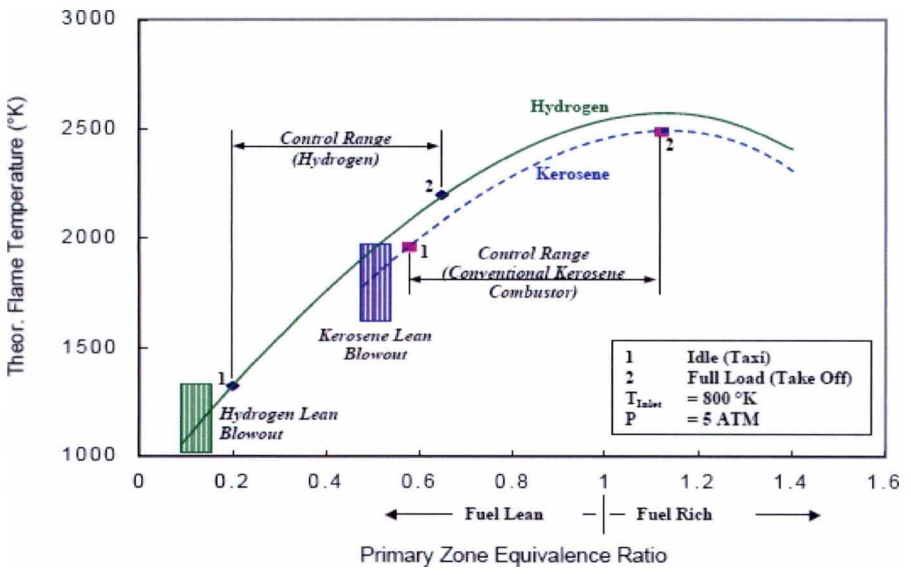

Fig. 19 Temperature characteristics H2/Kerosene combustion (from [31]).

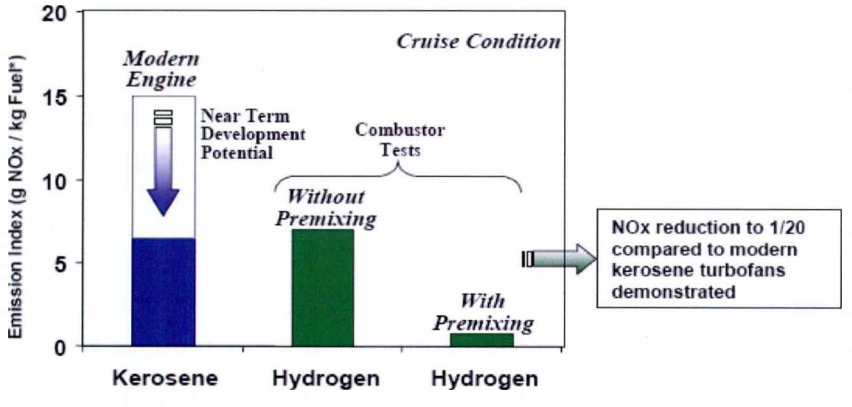

Fig. 20 Comparison of NOx emission for a gas turbine test setup applying H_2 or kerosene (from [31]).

According to [31] a twenty fold reduction in NOx emissions (as compared to modern kerosene combustor technology) was demonstrated with a lean premix configuration as shown in Fig. 20. The higher flame velocity of hydrogen, in comparison with kerosene, would allow a shorter combustor length with potentially lower NOx levels. A drawback with the higher flame speed of hydrogen is the increased risk for flashback.

The matters of H_2 fuel generation, supply and system infrastructure is out of scope of the ATLLAS project. Accordingly the related safety questions are only briefly considered. It could anyhow be appropriate to sum up the key physical properties of hydrogen with respect to design and safety (as given in ref. [32] compared to gasoline, natural gas, and propane):

Gaseous hydrogen:

- *density* – Hydrogen is the lightest of all the elements.
- *buoyancy* – At room temperature, gaseous hydrogen has a very low density compared to air
  and the other fuels. If it were to leak from a container, it would rise more rapidly than methane, propane, or gasoline vapour and quickly disperse.
- *diffusion* – Although gas transport from diffusion is much less than gas transport due to buoyancy, hydrogen diffuses through air much more rapidly than other gaseous fuels.
- *color, odor, taste, and toxicity* – Hydrogen, like methane and propane, is a colorless, odorless, tasteless, and nontoxic gas.
- *flammability and flame characteristics* – The flammability of hydrogen, as a function of concentration level, is greater than that for methane, propane, or gasoline vapor. Unlike the others, however, hydrogen burns with a low-visibility flame in the absence of impurities. In fact, in daylight, a hydrogen fire is almost invisible.
- *ignition energy* – Hydrogen can be ignited by a very small amount of energy if its concentration is neither lean nor very rich. (and the humidity is low).
- *detonation limits* – Hydrogen is detonable over a very wide range of concentrations when confined. However, unlike the other common fuels, it is difficult to detonate when unconfined.
- *flame velocity* – Hydrogen has a faster flame speed than the other fuels if its concentration is neither very lean nor very rich.
- *ignition temperature* – Compared to the other fuels, hydrogen has a higher ignition temperature.

(adds by author:)

- *specific heat* – extremely high, i.e. unique possibilities to store heat and to be used in heat exchangers.
- *influence on steel* - penetrates into steel and leads to "hydrogen embrittlement" with the risk for material cracking to follow.

Liquid hydrogen (LH):

- *low boiling point* – LH (at atmospheric pressure) evaporates at -253°C.
- *ice formation* (i.e. internal condensation) – Because of its low temperature, vents and valves in storage vessels might become blocked by accumulations of ice formed from moisture in the air.
- *condensation of air* (i.e. external condensation) – Again, because of its low temperature, uninsulated lines containing LH can be cold enough to cause air on the outside of the pipe to liquefy.

- *continuous evaporation* – The continuous evaporation (i.e. boiling) of liquid hydrogen in a vessel generates gaseous hydrogen that must be vented safely to prevent pressure buildup.
- *higher density* – The slightly higher density of the saturated LH vapor might cause a hydrogen cloud to flow horizontally or vertically upon release if a LH leak were to occur.

(adds by author:)

- *storage (1)* – LH occupies more than three times the volume of the same energy equivalent in kerosene. (density around 0.07 kg/liter compared with 0.8 kg/liter, heating values 121 v.s. 43 kJ/kg)
- *storage (2)* – added energy cost to keep hydrogen liquid compared with kerosene

3.9 Air oxygen and nitrogen separation

In the research of RLV:s (Reusable Launch Vehicles) for orbital missions, several ACES - Air Collection and Enrichment Systems - have been outlined [33], [34]. The main idea behind these kinds of systems, is to enable a cheaper and recoverable launch vehicle for coming space shuttles. One considered way to reduce weight, and thereby manage a horizontal take-off and landing, is to collect pure oxygen (and store it as liquid oxygen - LOX) during atmospheric flight. This LOX would then be used for rocket propellant combustion when leaving the atmosphere in the second phase take-off.

In the ATLLAS case the oxygen collection would not be a goal, instead one would like to have an: "air in $\Rightarrow$ O_2 + N_2 out" system running in steady-state. In such a case, following the O_2/N_2 separation, hydrogen would be burnt with almost pure oxygen in a core channel, while nitrogen is bypassed in an outer duct. With the N_2, ideally, not present in the combustion chamber, nor heated to critical temperatures, the NOx-problem would be gone!

The H_2-fuel, with its extremely high heat capacity, is very well suited as cooling medium in such a system, where also the needed heating of the hydrogen prior to combustion would be achieved in the same process.

Of course such a system would need a certain transition time, where NOx would be generated, when going from air to pure O_2 combustion (involving control of complex heat exchangers and active channel systems). Even in a "O_2 " combustion phase the purity would never get to 100%, let us assume a content of 90-99% O_2 , while the rest would be N_2 contaminations. Assuming that such a system overall is feasible, it could give a possibility to limit NOx generation to acceptable levels.

Central questions for such a feasibility study would be:

- the degree of oxygen purity (or nitrogen "contamination") needed in the core /combustion flow in order to reach acceptable NOx levels

- the size and weight of such a 'distillation – heat exchange system', capable of producing enough amount of O_2 for in-flight steady state conditions, including related aerodynamic consequences
- the over all efficiency of such a system involving the extra energy cost for the distillation and heat exchanger system (the gain in combustion efficiency when running on "almost pure" O_2 , related to the expected tremendous pressure/energy losses that can be expected from the distillation-separation system including outlet of N_2)
- the heating[13] and expansion/exhaust of N_2
- requirements on materials in the combustion chamber in order to withstand the extreme temperatures achieved
- system design allowing for a transition between a "conventional" RAM-jet air combustion engine, into a "nitrogen by-pass RAM-jet" with pure oxygen combustion.

Leaving all these matters of practical implementation aside, this air into nitrogen-oxygen separation approach was addressed in a small chemical kinetics study within ATLLAS WP 4.6. It was found that assuming: 1) residential times as short as 1 ms (which might be unrealistically short as discussed later), 2) N_2 separation prior to combustion, down to 1% of original N_2 content of air, a significant NOx reduction could be achieved. But: the resulting EINOx levels would still be far above the aimed 15g/kg!

[13] up to non-critical temperatures regarding NOx for the N_2 "contamined" with a small amount of O_2

4 NOx emission prediction methods

Detailed prediction of NOx emissions of hypothetical combustors is still beyond today's physical understanding and modeling capabilities. Though, estimates of NOx for an aircraft engine might be carried out with several kinds of methods, differing in their approach, complexity and accuracy. An attempt to categorize the main methods is given below.

4.1 NOx emission correlation methods

The principle of these methods is to define characteristic parameters, to which emission indices can be correlated with reasonable reliability. Several correlation methods can be found in the literature. There are basically two types of methods: direct prediction and relative correlation.
The direct methods usually consist of a formula which correlates EINOx to a certain set of characteristic engine parameters. To achieve most accurate results, the coefficients of these parameters have to be adjusted on the basis of measurements data for the given engine type of concern.
The relative correlation methods have been developed to overcome the restrictions of the direct prediction methods. They usually rely on publicly available data like emission indices and fuel flow data from the ICAO engine exhaust database [18]. On the base of these data, reference functions of EINOx of one or more characteristic parameters are developed. These functions are valid throughout the operating range of the respective engine and allow calculation of EINOx with satisfactory accuracy for any operating condition [35].
Both the above approaches are widely used for current turbofan engines but are, because of well-known reasons, lacking correlation data for RAM-jets and turbo jets.

4.2 Chemical equilibrium

Knowing the thermodynamic state and initial components of a gas system permits one to obtain the chemical equilibrium[14] compositions of the system. One example of a possible application of these methods, applied in ATLLAS WP 4.6, is the air-fuel combustion/NOx generation:
Given an initial combustion composition of air and fuel and the state of the mixture, i.e. the two thermodynamic state variables enthalpy and pressure, with

[14] the state in which the chemical activities or concentrations of the reactants and products have no net change over time. Usually, this would be the state that results when the forward chemical process proceeds at the same rate as their reverse reaction. The reaction rates of the forward and reverse reactions are generally not zero but, being equal, there are no net changes in any of the reactant or product concentrations

the assumption that no heat or work interaction with the surroundings occurs, the enthalpy of the final combustion products will be the same as for the initial reactants. By this approach, which involves the solution of a set of algebraic equations, one gets as a result the final adiabatic flame temperature, as well as the amount of final combustion products (including NOx). This can be regarded as a fair approximation of the process in a combustion chamber, involving also an assumption of a perfect micro mixing of fuel/air prior to the combustion. Beside the limitations settled by the above assumptions, an equilibrium analysis is lacking information about the time scale. The only thing we know is that the composition of reactants resulting from the analysis is the chemical species composition that would give the lowest bounded chemical energy (Gibbs energy). In most cases this is similar to the result given by reactions going on for ever. In this sense results from such an analysis constitutes an upper limit of the combustion production of NOx (note that the NOx production is much slower than the combustion itself).
This method has been applied for NOx emission estimations for both the ATTLAS M3Tand M6T concept in cruise. The computer code used are the NASA Gordon McBride code [36] and "HAP" [37] (the last one is basically a limited version of the Gordon McBride code specialised for RAM/SCRAM-jet combustion and thermodynamics) .

4.3 Chemical kinetics

In chemical kinetics one brings in also the chemical reactions and the rates of these processes. While chemical kinetics is concerned with the rate of a chemical reaction, thermodynamics and equilibrium chemistry determines the extent to which reactions occur. In order to compute the reaction products accurately one needs to have a sufficient set of reactions, with corresponding rate constants established. Also here the mixture and reactions are considered as homogenous in space. Such, more or less established, reaction sets might be found in the literature.

This method has been used for the M6T configuration for cruise conditions (hydrogen/air combustion). The applied chemical kinetics code was Kintecus [38]. An attempt to find reaction sets for the kerosene combustion in the M3T configuration case, and run Kintecus for this, failed and only chemical equilibrium studies were applied here for NOx level considerations.

4.4 Computational Fluid Dynamics (CFD)

In this case CFD, i.e. numerical gas flow modeling, is added to the thermal and chemical modeling. CFD in combination with reaction chemistry and advanced combustion/mixing physics and modeling (including ignition processes, turbulent combustion, flame modeling, ...) is to day a necessary set of tools in supporting the development of new aeroengine combustors. For fluid design

calculations, it is enough to get the values of density and temperature correct, and so fairly simple chemical mechanisms may be employed, with good results. However the prediction of trace species, such as NOx, requires the use of a significantly more complex kinetics scheme, with the resulting increase in computational effort required to solve the problem. Due to the different timescales involved, in combination with the need for a high spatial resolution, models and CPU-times become very large. In order to carry out CFD-computations, one would need information about the design details of the combustor, which are not at hand in ATLLAS. And further, as mentioned in the beginning of this paragraph, modelling solely is yet not enough to get accurate NOx data even for already existing jet engines, with all needed parameters known in detail.
CFD methods has not been applied for combustion/NOx simulation within ATLLAS, were instead the more comprehensive approaches reviewed above have been used in order to get approximate figures and trends of possible NOx emissions.

5 NOx prediction studies and results

5.1 General scope – cruise NOx

As stated above, the RAM-jet cruise phase NOx emissions are considered to be the most critical part for a SST as is the case for both ATLLAS concepts. This is further emphasised by the fact that other studies anticipate good possibilities to reach EINOx values around 15g/kg fuel for combined cycle turbo jets [25]. In line with this, the conceptual study of the HISAC project optioned also for a LPP combustion low-NOx methodology as an applicable low-NOx concept. Assuming that during the LTO cycle and turbo-jet phase the NOx can be acceptably solved by already existing or mid-term technology, the natural objective of the ATLLAS project is focused on studying the cruise phase NOx emissions and ways to reduce these.

5.2 Inherent limitations in applied methods

As indicated previously, the NOx studies herein, independent of the computational method, does not involve the fuel/air mixing process or the detailed combustion or flame properties. The chemical kinetics analyses represent originally one-dimensional (species concentration as a function of time) adiabatic chemical batch reactions for a perfectly micro-mixed gas mixture.

Incomplete mixing/fuel-consumption or heat transfer might though be introduced by means outlined further down in the text.

Some other general restrictions of the chemical kinetics analyses include:

- H_2 in the perfectly micro-mixed fuel/air-mix, in combustion examples, is as well as the air assumed to have been heated to the compressed air-temperature at the combustor inlet (typically around 1500 K for M6 conditions) i.e. the matter of energy losses due to fuel evaporation before its entry into the combustion chamber, is not included (this needed heat exchange might be used for combustor chamber liner cooling).
- The general geometry and length scale, of the engine and engine combustion chamber is not known and basically left outside computational results considerations.
- Though some baseline figures and assumptions have been applied in order to relate the chemical kinetics results to realistic physical configurations. These figures/assumptions are:

  1. The (mean axial) Mach number in the combustion chamber is assumed to be 0.5. This enables one to relate time to a space variable, the x-axis (this simple initial approximation is regarded to

be adequate enough in this context where we are aiming for general conclusions).

2. The NOx values of interest are those emitted to the atmosphere, i.e. those found in the nozzle exit, pos.10 in Fig. 21. Since these are a result of a very fast expansion from pos. 4 the NOx levels in these two positions have been assumed to be frozen in pos 4. I.e. the estimates of emitted NOx from chemical kinetics calculations has been taken from a state more alike the one in pos.4. Further, this has been done with an assumption of constant pressure within the combustion chamber.
3. In chemical equilibrium computations equilibrium NOx levels at the throat position (pos.8 below) represents the exhaust NOx.

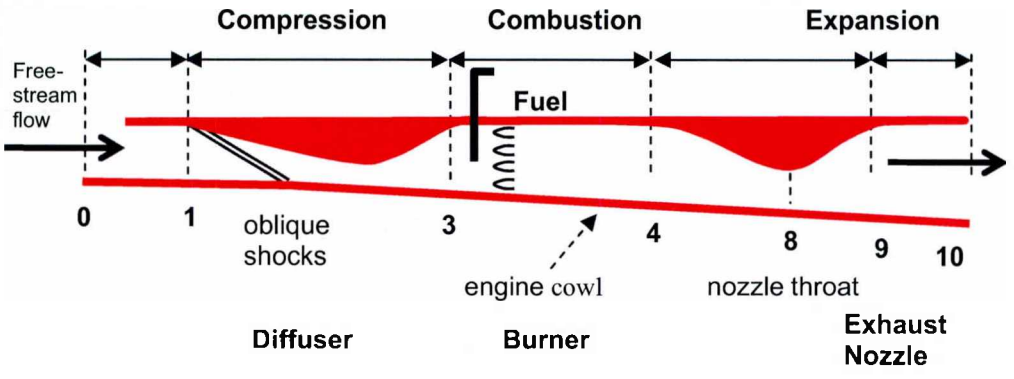

Fig. 21 RAM-jet principle layout with station numbering.

5.3 MT6 baseline conditions

The MT6 "black-box" RAM-jet baseline data was given from WP2 [39] and is summarised in Table 1 below (static values, at pos 3 ≈ total values since M ≈ 0). Position 3 is found at combustor inlet, and pos.4 at combustion chamber end, as seen in Fig. 21.

Table 1 M6T combustion baseline data (mass flows in kg/s, nozzle throat area in m^2).

M=6.0	$V_{freestream}$= 1800m/s		Alt.= 27 300m		stoichiometric Fuel to Air Ratio (mass) , fs= 0.42					
throttle	η_c	T3(K)	P3(bar)	T 4 (K)	P4(bar)	Mass-flow 3 (air)	Mass-flow 4 (air+fuel)	FAR (mole) f	ER Ø= f/f_s	Nozzle throat Area
100%	0.9675	1583	20.37	2800	18.55	411.6	424.1	0.44	1.05	0.34
32.2%	0.9675	1583	20.37	2125	18.63	419.4	424.5	0.175	0.42	0.279
100%	0.95	1583	14.54	2800	13.24	411.5	424.1	0.44	1.05	0.477
27.8%	0.95	1583	14.54	2125	13.30	419.4	424.5	0.176	0.42	0.39

It should be noted here that for all chemical equilibrium studies the compression efficiency η_c for the intake is set to the highest value 0.9675 of Table 1 which gives a combustor inlet pressure of 20.37 bar.

5.4 Baseline M6T chemical equilibrium simulations

Outgoing from the Table 1 M6T baseline data the Gordon-Mc Bride chemical equilibrium code (CEA) was run. The code was run in "Rocket problem"[15] mode which allows for a simultaneous computation of chemical composition and thrust related data. In our case the fixed input was nozzle/combustor chamber ratios, combustor inlet temperature and pressure. In order to get the wanted inlet air mass flow, 1630kg/s (408kg/s per engine, given by inflow at cruise velocity 1800m/s at 27.3 km altitude standard atmosphere) some iterative steps was needed in order reach the correct nozzle throat area. The final thrust for each case were approximated in a 1D-model as: $T=mdot_eV_e-mdot_oV_0+(p_e-p_0)A_e$, where subscript e denotes the engine exhaust exit section, which corresponds here to the x-wise position at the fuselage trailing edge, and 0 denotes the free stream values. A_e is the projected area of nozzle/fuselage expansion surface as seen in Fig. 23, $A_e = 46.4\ m^2$ (mdot=mass flow, V=velocity and p = pressure).

In order to get a complete dataset of defined input variables for a "Rocket problem" also the combustion chamber end cross section area, A_c, has to be given. Based on the external geometry of the baseline M6T this was set to 6 m^2.

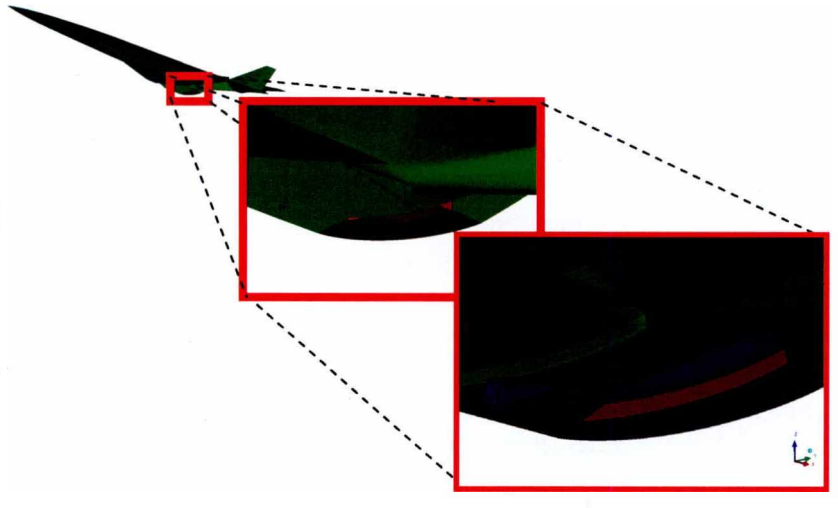

Fig. 22 **M6T nozzle region with nozzle throat shown in red and rear part of combustion chamber in blue (in the right most figure surfaces are shown as transparent).**

[15] The "Rocket problem" mode in CEA allows for computation of thermodynamic state properties along the nozzle as well as chemical composition (e.g. NOx content) for finite-area combustors given the combustion inlet states. This is for any given gas mixture and area relation – i.e. combustion chamber end v.s. nozzle throat, or at any other position between the throat and the nozzle exit, assuming combustor inlet velocity ≈ 0. The chamber in the model is assumed to have a constant cross-sectional area. In this chamber combustion is a non-isentropic, irreversible process. During the burning process, part of the energy released is used to raise the entropy, and the pressure drops. Expansion in the nozzle is assumed to be isentropic

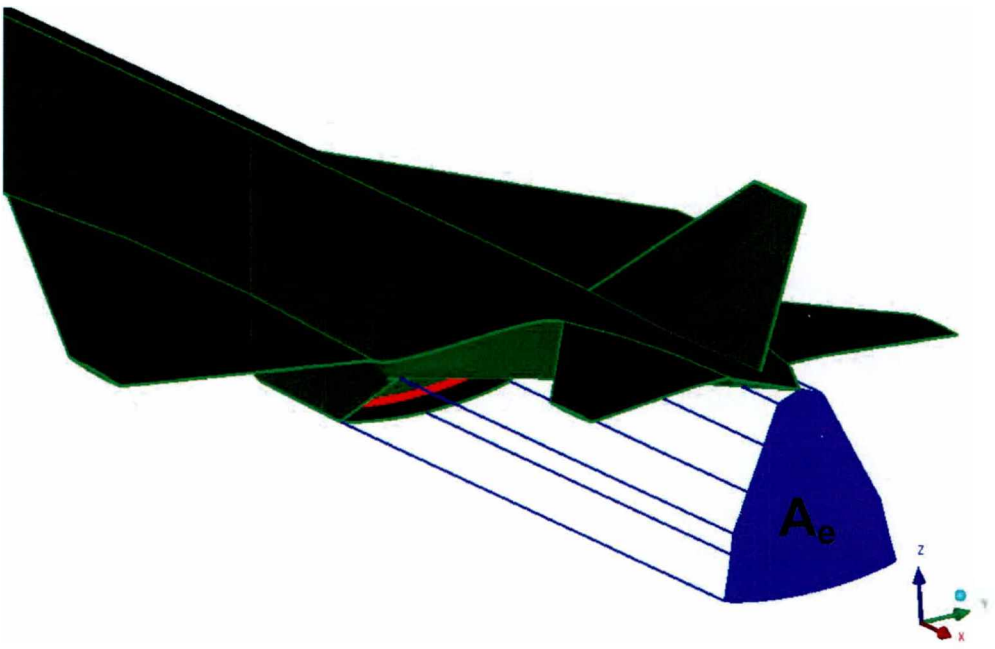

Fig. 23 M6T nozzle region with nozzle exhaust section defined as the blue projection (x= const.) area (nozzle throat in red).

The baseline configuration was run for different equivalence ratios and two different values of intake (or compression) efficiencies, η_c=0.9675 and η_c =0.95. Together with NOx emissions (NOx concentrations, EINOx and mass of NOx) also thrust and propulsion efficiency results were derived from these computation. The combustor inlet temperatures where set to 1583 K for both for the air inflow and the H_2 fuel (as given by DLR as nominal cruise input), except for one case where the H_2 inlet temperature was set to 500 K [16]. The equivalence ratio was varied between 0.25 up to 2. The results from these simulations are summarised in table 2 and 3 below (not shown here is that the resulting the nozzle exit Mach number, as defined above, is found in the range of M=4.25 to 5.4). NOx values are taken from the nozzle throat. This approach gives slightly lower levels than equilibrium values than if taken at the combustor chamber end. As discussed later on in paragraph 5.6 these nozzle exit values most probably constitutes under-estimates of NOx (due to the limited time in the fast expansion to reach equilibrium).

[16] a more representative fuel inlet temperature (for a RAM jet engine) could be somewhere in this range, i.e. between 500 to 1583 K. But since no drastic NOx variations, or resulting exhaust temperature, were found by varying the inlet fuel temperatures within this range (27% in NOx, 9% and 14% respectively in thrust and thrust-power, see below) fuel combustor inlet temperatures were kept at 1583 K throughout most of the studies for the M6T (air inlet temperature T_3 held constant at 1583 K throughout).

Table 2 Baseline M6T NOx and efficiency data equilibrium simulation Results for $\eta_c = 0.9675$

η_c=0.9675 T_3=1583	p_3=20.37bar mass flow air=1629 kg/s								
EMISSIONS Ø	0.15	0.25	0.5	0.75	0.9	1	1.25	1.5	2
EINOx	1134	1285	1459	1113	751	520	180	68	14
wEINOx	403	457	519	395	267	185	64	24	5
gNOx/s	5166	9773	22102	25139	20266	15561	6687	3022	838
wgNOx/s	1836	3473	7855	8934	7202	5530	2377	1074	298
molefraction (%)	0.31	0.55	1.20	1.30	1.00	0.76	0.31	0.13	0.03
A* (m^2)	0.93	1.00	1.16	1.27	1.33	1.36	1.42	1.46	1.53
Tthroat (K)	1741	1961	2419	2750	2880	2930	2944	2874	2758
Texit (K)	331	410	625	849	988	1082	987	925	831
THRUST Ø	0.15	0.25	0.5	0.75	0.9	1	1.25	1.5	2
mdotFuel (kg/s)	6.89	11.48	23.06	34.42	41.34	45.91	57.35	69.01	91.62
F , inst.Thrust (kN)	342	611	1200	1680	1950	2100	2230	2340	2540
Fp , pressure Thrust (kN)	-4	10	48	85	109	126	119	119	119
Fvo , ThrustPower (kW)	6.2E+05	1.1E+06	2.2E+06	3.0E+06	3.5E+06	3.8E+06	4.0E+06	4.2E+06	4.6E+06
mdot*hpr, chemEnergyRate(kW)	8.3E+05	1.4E+06	2.8E+06	4.1E+06	5.0E+06	5.5E+06	6.9E+06	8.3E+06	1.1E+07
Engine Mech.Power m'eVe^2/2-m'oVo^2/2 (kW)	6.4E+05	1.2E+06	2.4E+06	3.5E+06	4.2E+06	4.6E+06	4.9E+06	5.2E+06	5.7E+06
EFFICIENCIES Ø	0.15	0.25	0.5	0.75	0.9	1	1.25	1.5	2
ηo (over all efficiency – FVo / mdotf*hpr)	0.74	0.80	0.78	0.73	0.71	0.69	0.58	0.51	0.42
ηth (thermal efficiency – EnMechPow / mdot*hpr)	0.78	0.85	0.87	0.86	0.84	0.83	0.71	0.63	0.52
ηp (propulsive efficiency – FVo / EnMechPow)	0.95	0.94	0.90	0.86	0.84	0.83	0.82	0.81	0.80

It may be noted here that the seemingly good gNOx/s-results for fuel rich fuel-to-air ratios could be misleading, if not accounting for the fact that a large quantity of the H_2 fuel would stay unburned (because there is not much O_2 left for creating NOx in the combustion chamber). Though, the trend reveals a potential for the RQL-combustion principle for lower NOx. To make the comparison even more straightforward, one should also divide the value by the flight velocity (or Mach number) to assess the NOx emission per unit distance flown.

Table 3 Baseline M6T NOx and efficiency data, special low H_2 temperature case. Input as above, equilibrium simulation results for η_c=0.9675, Ø=1, etc, but T3 H_2=500 K

Ø =1 T3, AIR=1583, H_2=500 K							THRUST DATA						EFFICIENCIES		
EINOx	wEINOx	gNOx/s	Mole Fraction (%)	A* (m^2)	Tthroat (K)	Texit (K)	Mdot Fuel	F (kN)	Fp (kN)	Fvo (kW)	mdot*hpr	Engine Mech. Power (kW)	ηo	ηth	ηp
375	133	11233	0.55	1.32	2796	954	45.95	1.900	107	3.5E+06	5.5E+09	4.09E+06	0.63	0.74	0.85

Comparing EINOx values for the two different fuel inlet temperatures (1583 vs. 500 K) at ∅=1 from Table 2 and Table 3 reveals a NOx reduction of 27% related to a thrust reduction of 8.6% and thrust-power reduction of 13.7%.

Table 4. Baseline M6T NOx and efficiency data equilibrium simulation results for η_c =0.95

η_c=0.95 T_3=1583 p_3=14.54 bar mass flow air=1619 kg/s				
EMISSIONS ∅	**0.25**	**0.75**	**1**	**1.5**
EINOx	1283	1097	525	75
wEINOx	456	390	187	27
gNOx/s	9713	24628	15618	3309
Molefract (%)	0.554	1.281	0.768	0.143
A*	1.44	1.80	1.91	2.04
Tthroat	1960	2738	2908	2874
Texit	469	955	1209	1039
THRUST DATA ∅	**0.25**	**0.75**	**1**	**1.5**
mdotFuel (kg/s)	11.40	34.21	45.62	68.43
F (inst.Thrust, kN)	5.73E+05	1.61E+06	2.01E+06	2.25E+06
Fp (press.Thrust, kN)	2.47E+04	1.09E+05	1.54E+05	1.47E+05
Fvo (ThrustPower, kW)	1.03E+09	2.90E+09	3.62E+09	4.04E+09
mdot*hpr (chemEnergyRate)	1.37E+09	4.11E+09	5.47E+09	8.21E+09
Engine Mech.Power – (m'eVe^2/2-m'oVo^2/2 , kW)	1.05E+09	3.28E+09	4.21E+09	4.83E+09
EFFICIENCIES ∅	**0.25**	**0.75**	**1**	**1.5**
ηo (over all efficiency – FVo / mdotf*hpr)	0.75	0.71	0.66	0.49
ηth (thermal efficiency – EnMechPow / mdot*hpr)	0.77	0.80	0.77	0.59
ηp (propulsive efficiency – FVo / EnMechPow)	0.98	0.88	0.86	0.84

Some of the results as shown in Table 2 to Table 4 above are given in the following figures:

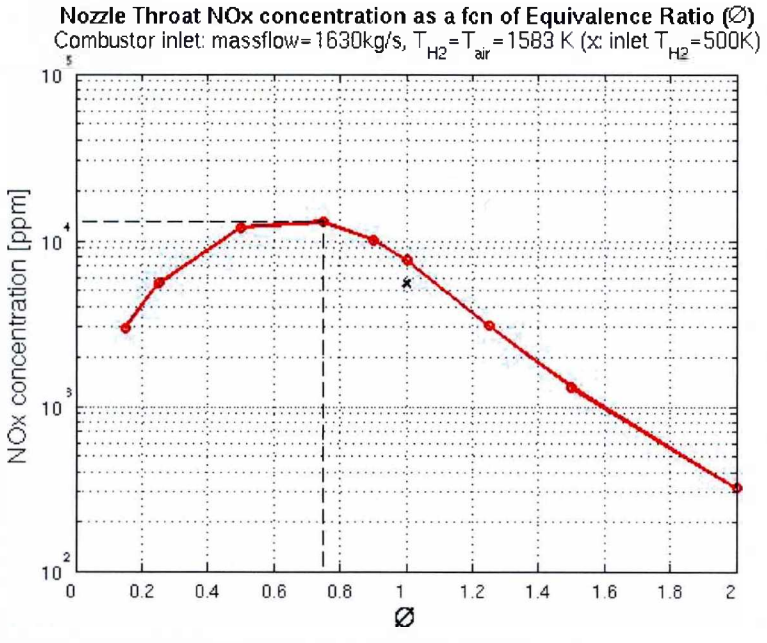

Fig. 24 NOx concentration as a function of ∅ (inlet compression efficiency and pressure has no discernable influence).

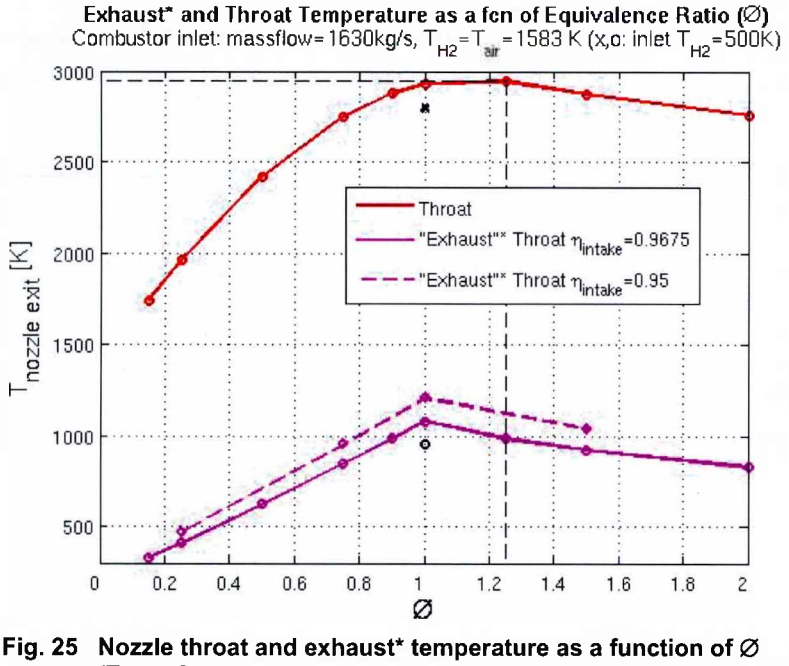

Fig. 25 Nozzle throat and exhaust* temperature as a function of ∅ (T_{throat} for η_c=0.95 not shown since they are in level with η_c=0.9675 as seen in Table 2.), *exhaust section as defined in Fig. 23.

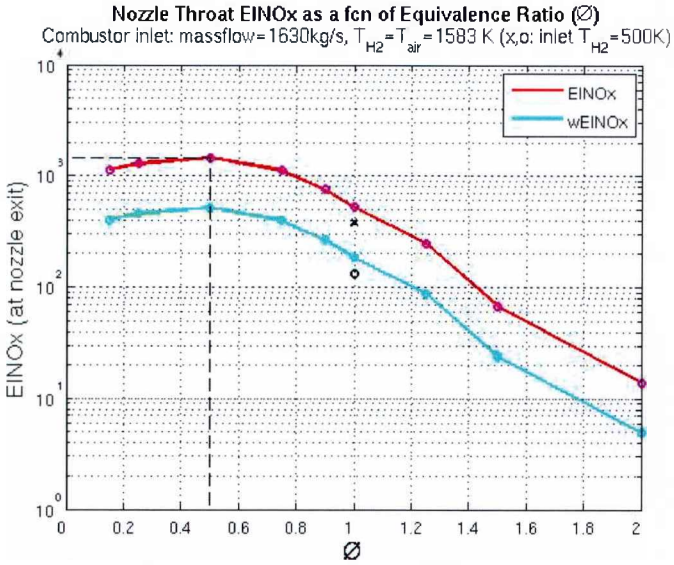

Fig. 26 EINOx as a function of ∅ from CAE runs
(Note: the relatively small changes from a decreased fuel inlet temp. x,o).

Continuing the results discussion with the NOx concentration variation with ∅, shown in Fig. 26, we see a peak NOx concentration at an ∅ close to 0.7 and a soft decline towards lower and higher ∅. The NOx production process is much slower then the combustion itself. At ∅=1 we get the fastest reaction times and equilibrium is reached in the shortest time (not seen here but in the chemical kinetics results to follow). Moreover we see that a reduction in combustor inlet H_2 fuel temperature from baseline level 1583 K to 500 K, reduces NOx levels only marginally.

In the following figures some engine performance and further NOx parameters from the equilibrium study are plotted.

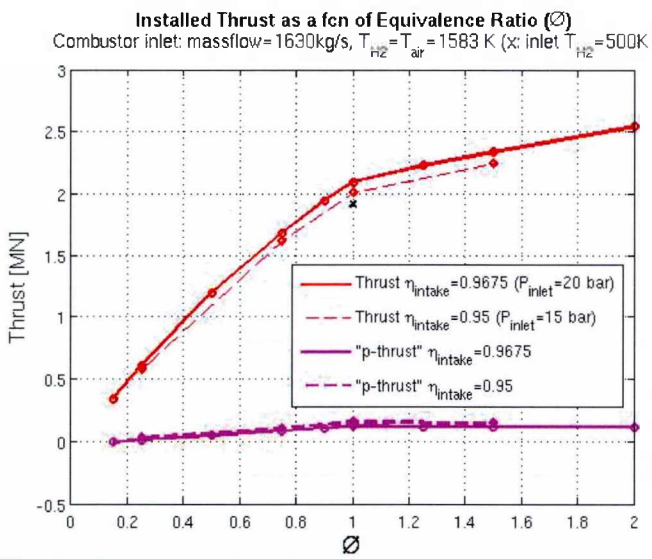

Fig. 27 Thrust as a function of ∅.

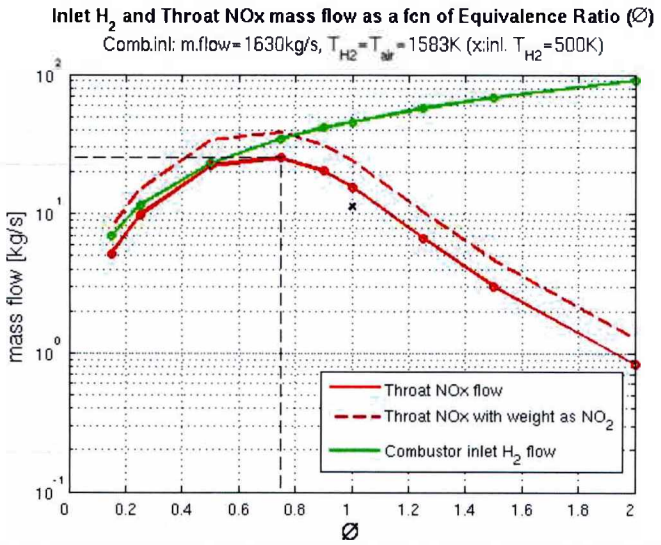

Fig. 28 Inlet H_2 and Throat NOx mass flow as a function of Ø.

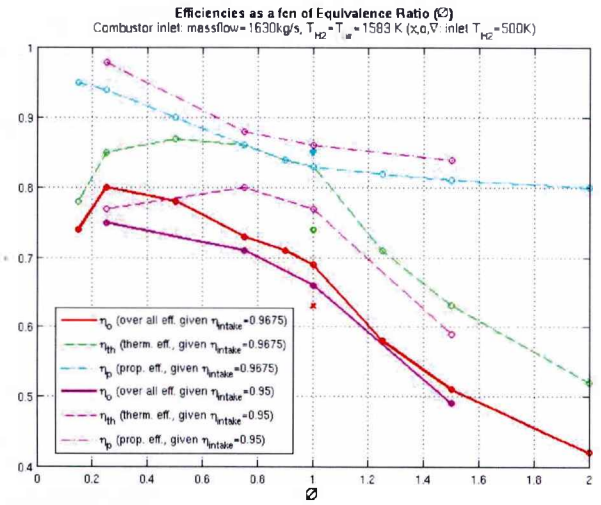

Fig. 29 Engine efficiencies as a function of Ø.

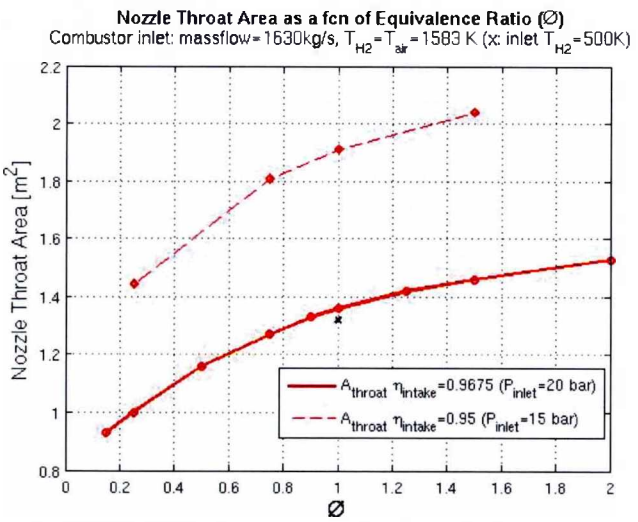

Fig. 30 Nozzle throat area as a function of Ø.

One should be aware that it is not possible to achieve an estimate of expected NOx levels for a RQL combustion from equilibrium results since the essential time information is lacking. Though, the equilibrium results give an indication of upper EINOx limits.

EINOx data in Fig. 26 indicate that we are very far from the 15 g/kg NOx that we are aiming for. EINOx(∅=1)=520 g/kg and a wEINOx, which could be better comparative estimate as discussed before, reaches 185 g/kg, i.e. more than 10 times this goal. EINOx peaks around ∅=0.5 keeping in mind that shortening residential times short enough, would never lead to these equilibrium levels. It can also be noted, in the same figure, that a temperature reduction of the combustor inflow hydrogen from 1583 to 500 K results in marginal changes of weighted EINOx values of 375 and 133 respectively (see "x"-mark in the figure, which denotes the results for a inlet H_2 temperature of 500 K).

In Fig. 27 one can see the fast degradation of estimated thrust with decreasing ∅, but, as seen in Fig. 29, related with this behaviour is also an increase in the overall efficiency which tend to peak around equivalence ratios close to 0.25. From this point of view it might be an idea to search for engine configurations able to run at lower ∅'s.
In this context, it is interesting to investigate Fig. 28 where the NOx and fuel mass flows constituting the emission indices are shown. For lower ∅ equilibrium mass flow levels of inlet fuel and outlet NOx are about the same giving EINOx levels around 1000.

Before going to the chemical kinetics, and trying to add a timescale to these reactions, the ATLLAS M3T and NOx are discussed.

5.5 M3T NOx equilibrium estimates

The M3T concept constitutes of a completely different approach regarding the propulsive system with a very large inlet mass flow and a very low (over all) equivalence ratio and temperature range. The baseline data in this case are (this is after after iterations during the project involving an increase in cruise Mach number from 3 to 3.5):

- Cruise M=3.5
- fuel kerosene (Jet-A)
- combustor inlet temperatures ($M \approx 0 \Rightarrow$ static cond. $\approx$ total cond.):
  T_{air}=750 K
  T_{fuel}=300 K
- distributed combustors – .i.e. only a part of the air flow is used for combustion, while the rest is by-passed and mixed with the combustion products.
- nozzle throat total conditions (assumed perfectly mixed combustion products and by-passed air): T=885 K, p=1.87

The equivalence ratio was iteratively changed, in runs with the Gordon-McBride code, until the wanted temperature of 885 K was reached. The final EINOx value for the given conditions then showed a value of 4g/kg fuel. This is reached for the extremely low, but still sufficient for needed propulsion, over-all equivalence value of 0.053.
Since only the over all design is defined, while the detail combustor geometry is not, this principal approach for the equilibrium analysis was taken. Nozzle total conditions, which constitutes an overestimation of temperature, and thereby also of NOx, were taken as input in the equilibrium analysis. But, the approach also involves an underestimation which can not be quantified (without going to chemical kinetics[17]). This NOx underestimation is due to the limited time, which in reality would be given, for the assumed perfect mixing and equilibrium to be achieved after the combustion in distributed local combustion zones.
Anyhow, from these indications one can conclude that the M3T case constitutes a very promising combustion concept regarding NOx, due to its relatively low working temperatures and equivalence ratio (except in the vicinity of combustion zones, from which the leaving combustion products could be assumed to be mixed and cooled with by-passed air rather quickly),. This is probably in line with already existing gas-turbine engines for which low NOx technology already exist.

[17] Initial attempts to run this case with chemical kinetics (for a reaction set of thousands of reactions and species) failed. Through communication with Terry Cain, Gas Dynamics Ltd /ATLLAS project, it was later concluded that a simplification, applying chemical equilibrium for the combustion phase only, and then starting out with these equilibrium combustion products + the by-pass air in a second step, could have been run with chemical kinetics. Unfortunately no time was left over for this study.

5.6 M6T chemical kinetics estimates

Before running specific M6T chemical kinetics cases a reaction set "Jachimowski" [42] was selected. This was initially tested against a few others (some also tested in LAPCAT II [22]) where it was found that they gave only a small difference regarding NOx, or in some cases the other comparative set failed to be run in Kintecus [38]. It should also be mentioned that the selected set was also run and compared with results, for the same input and reactions, given in ref. [38]. This comparison is shown in Fig. 31 below.

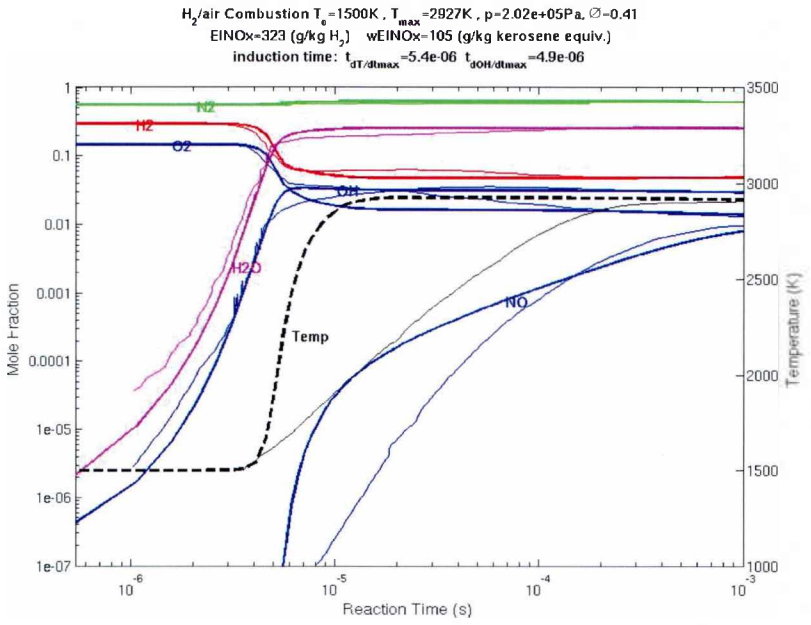

Fig. 31 Comparison of Kintecus H_2 combustion results with HAP[38] data (for the same input conditions and reaction set) Thick lines = Kintecus, thin lines = ref. [38].

We see here a good correspondence for the main species but not as good for NO, and quite a difference in temperature between around 0.01 to 0.1 ms. This temperature deviation can probably explain the deviation in NO, in the corresponding time range. The concentrations, as well as the temperature, achieved after 0.1 ms are in good correspondence though. The reason for this divergence is not understood. Nevertheless, Kintecus has shown good results for other testswhen compared with the more wide-spread code Chemkin. Since it includes well established thermodynamic databases it is believed to give trustworthy results.

For all chemical kinetics runs a simplification is made: the pressure is kept constant during the reaction time, i.e. the slight pressure and temperature drop through the combustion chamber is not taken into account, neither the fast expansion through the nozzle. This brings about a slight overestimation of NOx-levels.

5.7 Baseline M6T chemical kinetics results

The first ATLLAS baseline chemical kinetics results, with ∅ =1 shown in Fig. 32, reveals:

1. a very fast increase in NO concentration (NO_2 levels in the total NOx much smaller than in NO, as in chemical equilibrium computations)
2. equilibrium is reached already after ca 0.1 ms
3. a very high EINOx value of 720g/kg. This is in agreement with equilibrium results for the baseline , ∅ =1, results, which gave an EINOx=724g/kg at the injector (T=3132 K, P=20.37 bar) and at combustor end and nozzle throat 719 and 520 g/kg respectively. (temperatures 3127 and 2930K, and pressures 19.9 and 11.5 bar respectively).

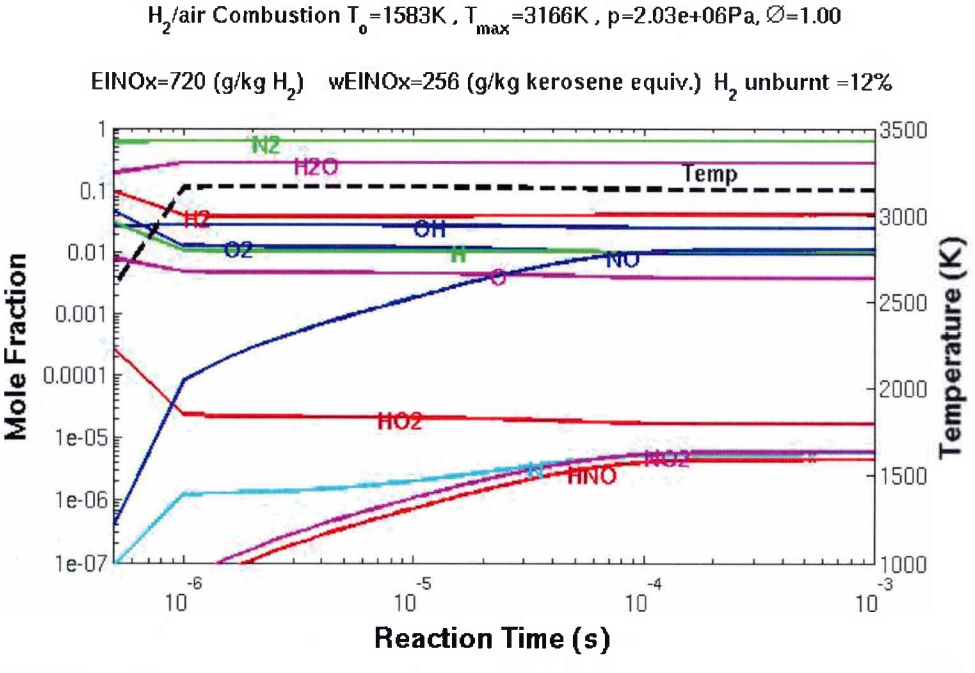

Fig. 32 Baseline species concentration equivalence ratio ∅ =1, H_2 combustion.

From the small change in NOx equilibrium values between injector and combustor end position, we can assume that the corresponding pressure and temperature drops would neither have reflected much change in NOx even in a chemical kinetics study , rather that the difference would have become smaller (not time enough to go down 5 g/kg). The same reasoning holds for the nozzle NOx levels in the equilibrium studies for the nozzle throat, were the flow is accelerated up to Mach = 1, i.e. previous equilibrium nozzle throat NOx values (given in Table 2) can be considered to constitute underestimations.

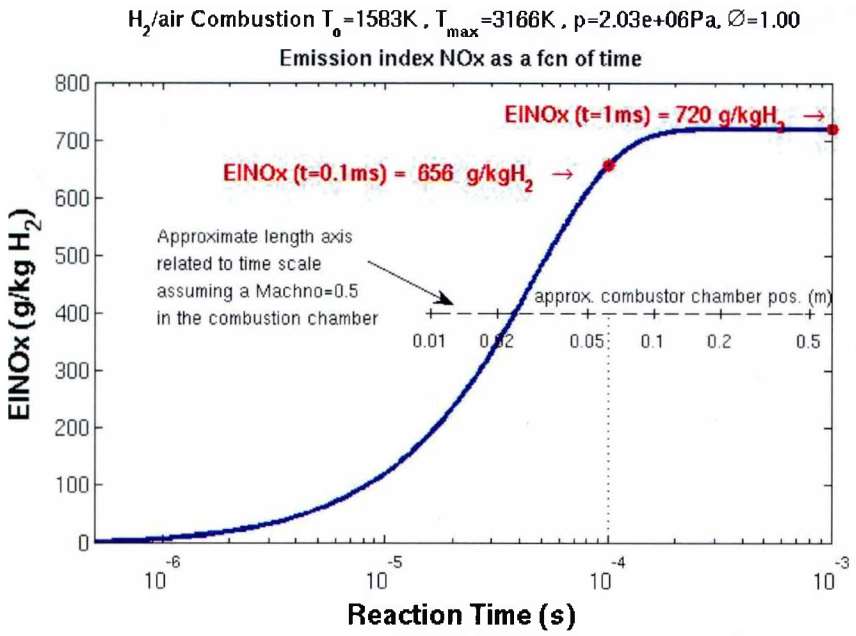

Fig. 33 Baseline EINOx development equivalence ratio ∅ =1, H_2 combustion..

In Fig. 33 the time history of EINOx is shown. It is clear that equilibrium values are reached already after approximately 0.2 ms. In order to get a rough estimate of what this means in terms of a length scale, a very approximate length scale is added into the graph. Knowing we have a Mach number between 0<M<1 within the combustion chamber, a M = 0.5 is set to generate this rough length scale. Given this, we find that an EINOx value of around 600 g/kg is reached already after a distance of 5 cm after the combustor (distance=0). Even with a velocity closing up to M = 1, we get the unrealistic short combustion chamber length of 10 cm, and in order to reach levels around the targeted 15 g/kg, the length would need to be in the order of a millimetre! With temperatures around 3000 K we have a sound velocity close to 1000 m/s , which means that the M = 0.5 and the time scale of 1 ms corresponds to length of not more than 0.5 m. Even this would probably constitute a too short combustion chamber but is taken as the reference for an absolute minimum combustor chamber length in the studies to follow. This may be motivated here because of two reasons, 1) we do not include the part of the chamber where mixing occurs and 2) The combustion time for hydrogen is much shorter than for kerosene which would give possibilities for shorter chambers.A reduction of fuel to the baseline conditions, ∅ =0.42, show only a slight reduction in NOx as seen in Fig. 34.

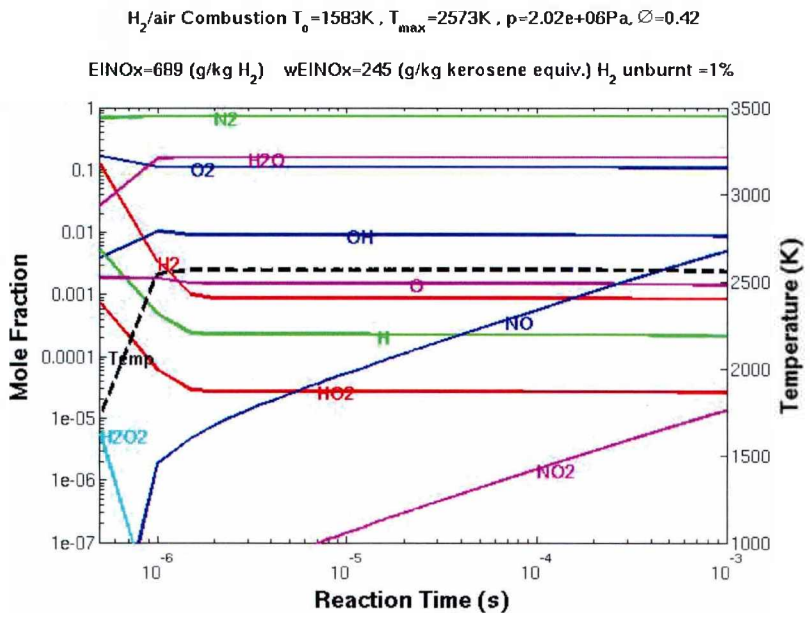

Fig. 34 Baseline species concentration equivalence ratio ∅ =0.42, H_2 combustion.

Compared with the ∅ = 1.0 case, we see that neither the NOx concentration nor the EINOx values change very much for this lower equivalence ratio. The NOx concentration is reduced about 50% while the EINOx value goes from 720 to 689 g/kg fuel (keep in mind the 60% less fuel for the ∅ =0.42 case). In the EINOx curve, in Fig. 35, we see that the EINOx increase, towards the end value of the simulation time, 1 ms, is much slower, almost a factor of 1/10 slower compared with the ∅ = 1.0 case (Fig. 33, note EINOx rate of change).

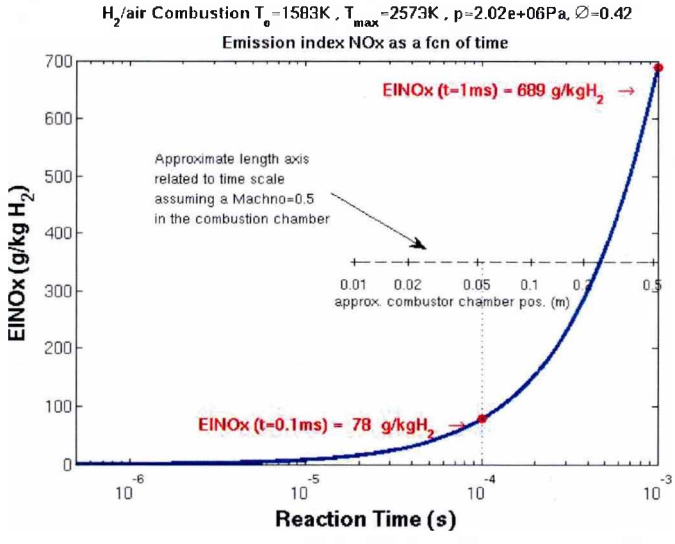

Fig. 35 Baseline EINOx development equivalence ratio ∅ =0.42, H_2 combustion.

Further, the EINOx value is still increasing at 1 ms, i.e. equilibrium not reached (in accordance with chemical equilibrium results, which shows a peak value around ∅ =0.5, see Fig. 26). But still unrealistically short chamber lengths are needed in order to reach EINOx values around 15 g/kg, i.e. in the order of 1 cm estimated for this case. One should here also note the reduced temperature, 2573 K against 3166 K, implying a strong reduction in efficiency (comparative values from equilibrium computations for ∅ =0.5 were 2671 , 2666 and 2419 K respectively for injector, combustor end and throat are well in line with this).

5.8 Variation of equivalence ratio

By running a few more equivalence ratios for up to a time of 1 ms we get a view of EINOx change when leaving the baseline ∅ (=0.42) , still with initial (total=static) conditions T_3=1583 K, p_3= 20.37 bar.

Table 5. EINOx , NOx concentration and T as a fcn of ∅

∅	EINOx g/kg at t=1 ms	NOx conc. (ppm)	T3 (K)
0.25	31	0.14e3	2233
0.42	689	5.0e3	2573
1.	720	10.9e3	3166
1.5	110	2.2e3	3217
2.5	7	0.18e3	2923

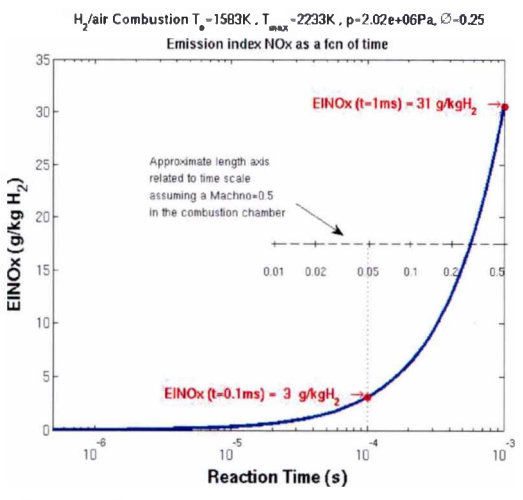

Fig. 36 ∅ =0.25 EINOx development.

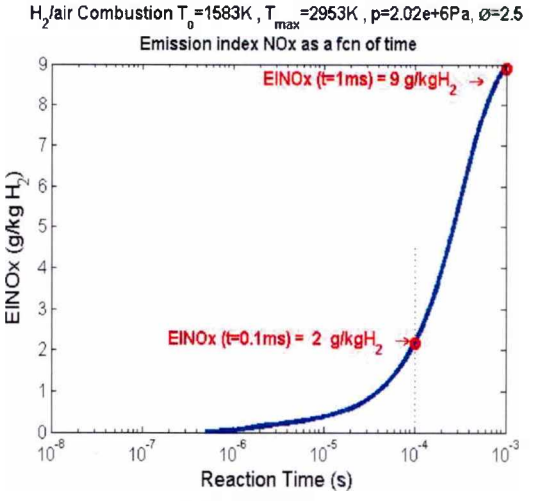

Fig. 37 ∅ =2.5 EINOx development.

The most significant figures to notice in Table 5 is the large decay in EINOx from ∅ =0.42 to ∅ = 0.25, where the EINOx value (taken after 1 ms) goes from 689 to 31 g/kg. This EINOx decrease is though a result of the accompanying lower temperature, going from 2573 to 2233 K, which strongly reduces the thrust. As found in previous chemical equilibrium study this thrust reduction can be estimated to 45% (from Fig. 27: 1.1 and 0.6 MN for ∅ =0.42 and 0.25 respectively). Still, EINOx values for the ATLLAS baseline, with equivalence ratios away from 1 show quite low levels which imply that a RQL combustion approach could be worth a study.

5.9 NOx reduction methodologies study

5.9.1 RQL example simulation

Starting out from the baseline data a RQL combustion, or a staged combustion in two steps, has been studied regarding NOx. The general input for this study was the air mass flow and combustor inlet states, T_3 and p_3, where pressure $p=p_3$, is assumed to be constant through the combustion process, as for the previous cases. The model is showed in Fig. 38:

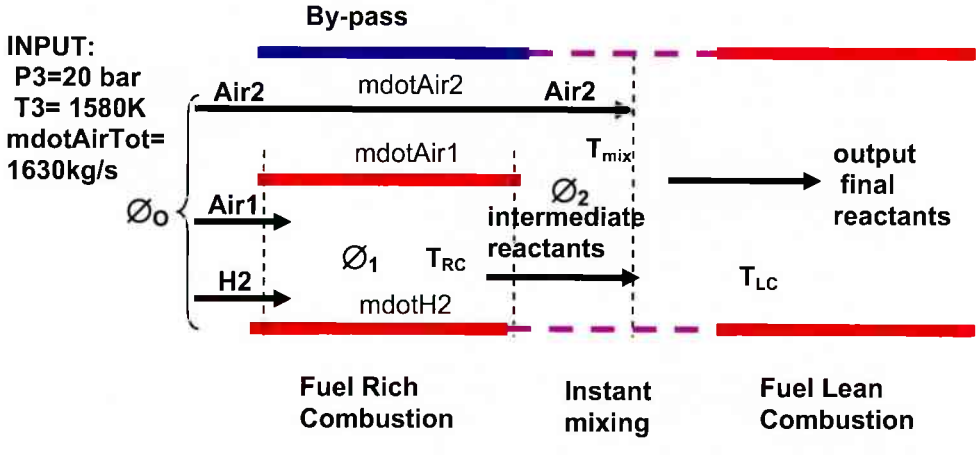

Fig. 38 Principal model for RQL simulation.

The input for the two-step staged combustion model is the overall equivalence ratio, $\varnothing_{OA}$, and the equivalence ratio $\varnothing_1$ for the first step (fuel rich combustion).. Cruise velocity is 1800m/s at 27.3 km altitude. The remaining properties needed are then given by (fs=stoichiometric fuel-to-air-ratio):

total air mass flow	mdotAirTot = mdotAir1+mdotAir2=1630 kg/s
fuel mass flow	$mdotH2 = \varnothing_{OA} \cdot f_s \cdot (mdotAir1+mdotAir2)$
rich combustion air mass flow	$mdotAir1 = mdotH2 / (\varnothing_1 \cdot f_s)$
rich combustion fuel + air mass flow	mdot1 = mdotH2 + mdotAir1
by-pass air mass flow	mdotAir2 = mdotAirTot - mdotAir1

In chemical kinetics computations the fuel rich combustion is run in a first step giving the intermediate reactants as output with a resulting temperature. To this, first output species concentrations, is the by-passed air (mdotAir2) added. The temperature of this mix ("instant mixing" in Fig. 38 **Fig. 38**) is given by (Cp:s given from the Gordon McBride code):

$$T_{mix} = (Cp_{RC}(T_{RC}) \cdot mdot1 \cdot T_{RC} + Cp_{Air2}(T3) \cdot mdotAir2 \cdot T3) / (Cp_{RC}(T_{RC}) \cdot mdot1 + Cp_{Air2}(T3) \cdot mdotAir2)$$

where:

$Cp_{RC}(T_{RC})$ = Cp for the reaction components at the temperature before mixing with air

This mixed species concentration is then run in a second step at p = p3 = 20.37 bar and T = T_{mix}. The reaction time extent was set to 1 ms for each step. In the second lean combustion step an approximate equivalence ratio is given by Table 6:

Table 6. Equivalence ratio definitions in RQL study step 2 (lean stage).

Ø	based on	written out
$Ø_{2\_Air\_only}$	H_2 / by-passed Air only	mdotH2unburnt /(mdotAir2·fs)
$Ø_{2\_All}$	H_2 / (by-passed Air + Rich burn products – H_2)	mdotH2unburnt /(mdotAirTot·fs)
where: mdotH2unburnt ≈ mdotAir1·fs·($Ø_1$-1)		

Three different combined equivalence ratios were studied as seen in Table 7.

Table 7. RQL cases runs with EINOx results.

Case	$Ø_{OA}$	$Ø_1$	$Ø_{2\_Air\_only}$	$Ø_{2\_All}$	mdotAir1 (kg/s)	mdotAir2 (kg/s)	mdotH2 (kg/s)	mdotH2-unburnt (kg/s)	$T_{mix\ (K)}$	EINOx (over all) g/kg
1	0.39	2.5	0.28	0.23	254	1376	18.5	11.1	2440	**4300**
2	0.39	1.5	0.18	0.13	424	1206	18.5	6.2	2660	**3890**
3	1.0	1.5	1.0	0.33	1087	543	47.5	15.8	3074	**1540**

As seen all three cases giving a very disappointing EINOx result though the intermediate equivalence ratios, in at least case 1 indicated possible gains in EINOx as seen in Fig. 36 and Fig. 37 above. Though, we have to keep in mind that in the last step, lean burn of RQL simulation, all cases starts at a much higher temperature than in previous examples (i.e. 2440 K against 1583 K in case 1). The reason behind these very high EINOx levels, are believed to be a result of the too long residential time at high temperatures. The species concentration development in case 1 is shown in Fig. 39 and Fig. 40 below.

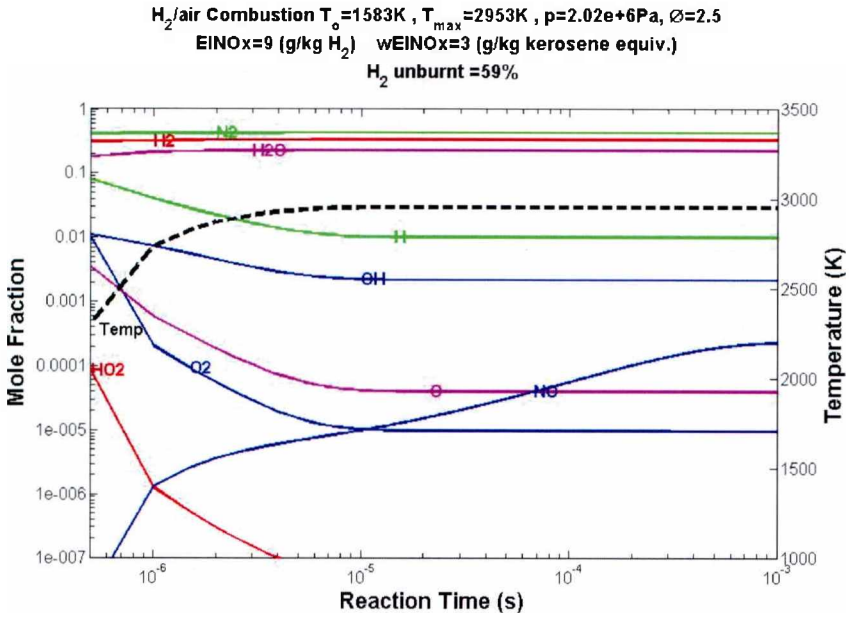

Fig. 39 Step 1 case 1 RQL, $\varnothing_1$= 2.5 (EINOx development see Fig. 37).

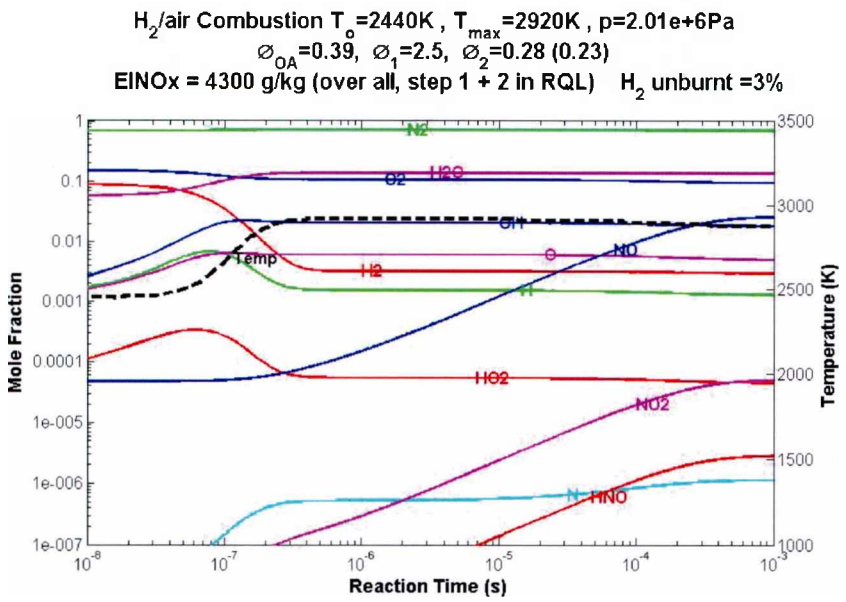

Fig. 40 Step 2 case 1 RQL, $\varnothing_2 \approx$ 0.28 (0.23), $\varnothing_{OA}$= 0.39.

As seen in Fig. 40 the NO concentration is flattening out towards equilibrium values in the lean combustion phase if the residential time for the second step combustion reaches values around 0.5 milliseconds. Given the baseline combustor inlet conditions, it seems that an "acceptable" NOx level is not possible to reach with RQL with realistic combustor lengths. This is the conclusion when taking into account results from all the three RQL simulation cases.

5.9.2 O_2 - N_2 separation

The question, if the more drastic approach of O_2 and N_2 separation (described in section 3.9) could enable a theoretical way to reach low-NOx, is outlined below. The analysis is based solely on quite simple chemical kinetic studies and leave matters related to the implementation and propulsive efficiencies aside. In initial equilibrium computations (not shown) it was seen that even an extremely low content of remaining N_2 (even levels of 0.01%) was not enough to create acceptable NOx levels. So, chemical equilibrium analysis and time histories had to be applied in order to find eventual possibilities of significant NOx reduction.
The first case is exemplifying a remaining part of 5% of N_2 (replacing the original air/fuel mix content of 75% N_2). The extremely high temperatures reached with almost pure hydrogen oxygen mixtures brings about a need to reduce the equivalence ratio (in this case: H_2 in relation to pure O_2 , versus stoichiometric ditto, i.e. stoichiometric fs=H_2/O_2=2). ∅ was in this example set to 0.17. Intake temperature was according to baseline data and intake pressure reduced to 1.26 bar (baseline 2.0 bar) in order to, in some way, account for the pressure losses linked with the separation of O_2 and N_2.

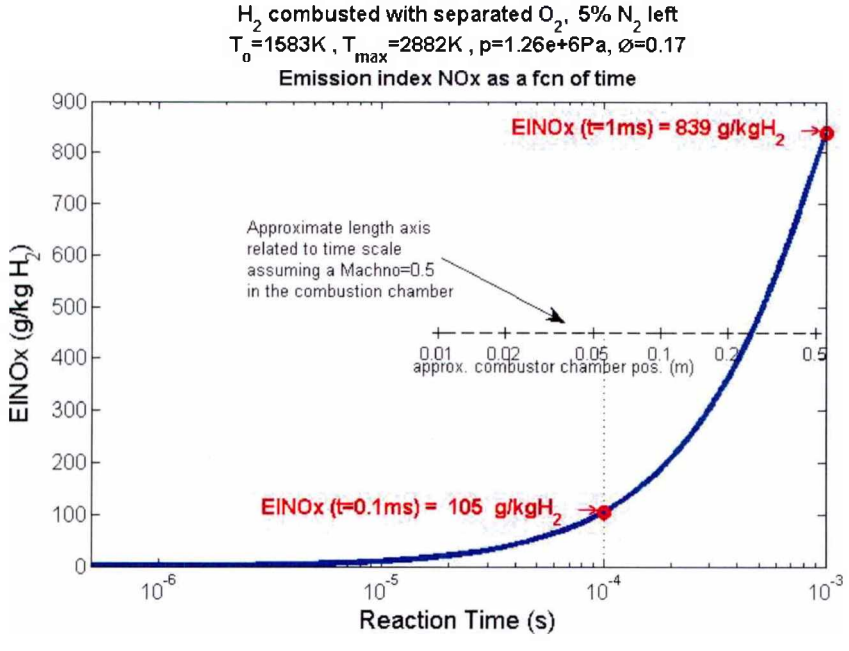

Fig. 41 O_2 and N_2 separation. Assumed 5% N_2 remaining.

As seen in Fig. 41 we are still far from the aimed ca 45 g/kg EINOx (or 15 g/kg wEINOx). The excess (unburned) oxygen and remaining N2 is obviously enough to produce these quite high amounts of NO. Again one may note that equilibrium is not reached.
The next case shows results for an assumed higher level of N_2 purity, 1% left.

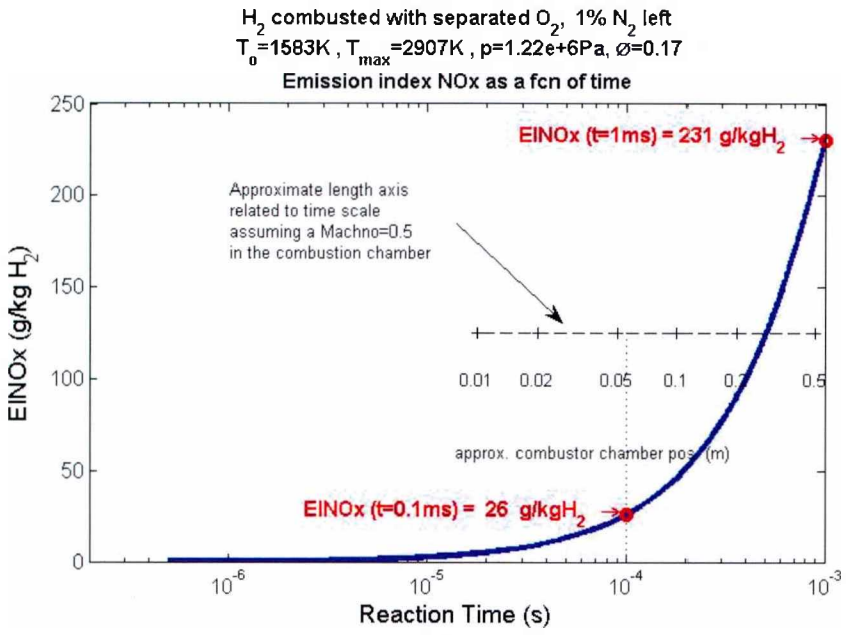

Fig. 42 O_2 and N_2 separation. Assumed 1% N_2 remaining.

The EINOx reached after 1 ms corresponds to a wEINOx of 82 g/kg H_2. The EINOx is still increasing after 1 ms as seen in Fig. 42. A significant reduction, compared with previous cases. But still, we are far away from the aimed 15 g/kg wEINOx which is reached already after about 0.2 ms (EINOx) ca 45 g/kg. Beside the extremely short distance, on which mixing/combustion would have to be carried out, we have also to take into account the by-passed N_2, which are not allowed to be heated too much in order not to generate significant NO.

5.9.3 Cooling

A cooling is simulated outgoing from the baseline case with ∅ = 1. It is very hard, even with flow, geometry and combustor material specifications given in detail, to come up with a good estimate of energy/temperature losses due to conduction and radiation. In our case an energy loss in mole-Kelvin/second was trimmed in order to reach a temperature decline from nominal ca 3170 K after 1.e-5 seconds down to ca 2900 K after 1 ms. This heat-sink corresponds to a value of 240 mol-Kelvin/second. The resulting NOx concentration plots are shown to get a picture of how fast NOx levels may decay for a relevant heat loss in the base line case, more than giving a precise NOx estimate for a specific system.

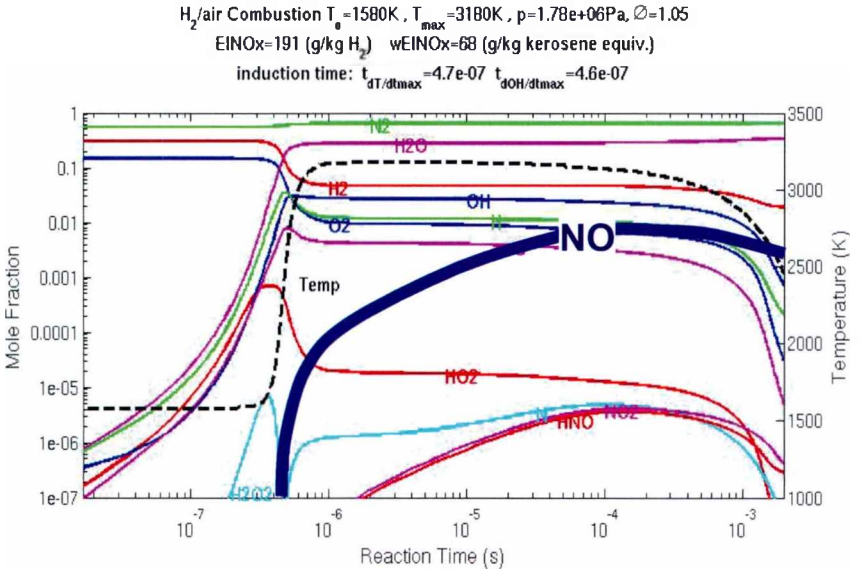

Fig. 43 Simulated cooling 240 mol-Kelvin/s Mole fractions, baseline with ∅ = 1.

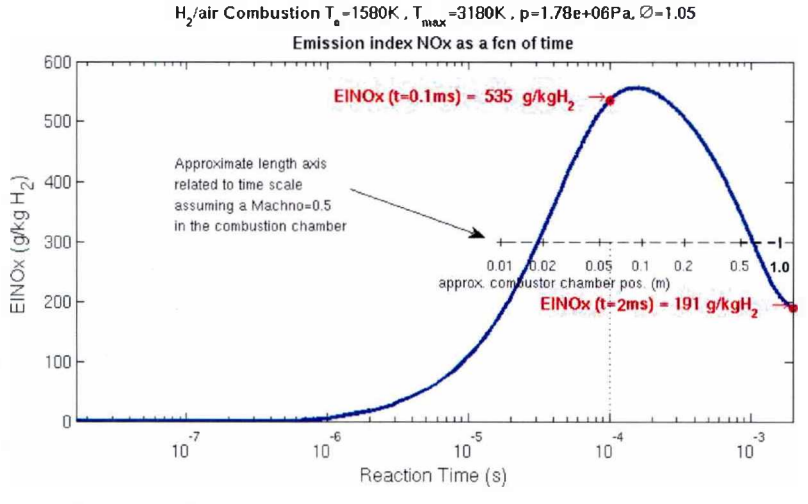

Fig. 44 Simulated cooling 240 mol-Kelvin/s EINOx, baseline with ∅ = 1.

Both Fig. 43 and Fig. 44 reveals a reduction in NO after that the cooling starts at $1.0 \cdot 10^{-5}$s reaction time. This decrease is accompanying the decreasing temperature which reaches a value lower than 2500K after 2 ms. However one should also account for a severe reduction in propulsive efficiency. NOx levels after this time interval are still considerably higher than the aimed 15g/kg wEINOx (68g/kg). As in the case where NOx increases with rising temperature, the NOx decrease is lagging the temperatures decrease. This behaviour points out the need to avoid high peak temperatures, as far and as late as possible. A low NOx combustion should preferably be searched in a "short residential time concept" rather than by cooling. Some of the other species are shown to decay at a much faster rate than NO which also shows a tendency to level out after 2 ms.

5.9.4 Water injection

In an attempt to get an indication of what could be achieved with water injection into the RAM-jet combustion zone, a case was studied with the inlet temperature set to 1500 K (baseline 1583 K). The resulting NOx and combustor exit temperatures are listed in Table 8.

Table 8. Results from combustion with added water.

H_2O added (% in moles of H_2)	wEINOx	T4 (K)	ΔT4(K)
0	192	2927	-
10	162	2889	-38
40	87	2796	-131

The result reflects basically NOx variations previously seen in direct variation with temperature. Considering the amount of water to be carried by the aircraft in order to reach significant NOx reduction the approach of adding water (10% mole content equals 1.8 times the weight of H_2 fuel!) can be regarded limited or impossible.

5.10 Comparison with A380 cruise NOx emissions

Outgoing from the above M6T baseline data a rather simple, but still informative, comparison with cruise NOx might be made. The comparative aircraft chosen is the Airbus A380, which can be considered to be the cutting edge regarding NOx emissions of today's long distance flights. Aiming at an estimate of total NOx emitted for a intercontinental flight by A380 and the ATLLAS M6T concept the following input has been used [40],[41]:

A380

Fuel consumption/passenger and 100km, fc	3 liter/(pass. and 100km)
No. off passengers, nofp	555
Cruise speed, Vc	900km/h
Fuel weight/l, wf	0.8 kg

which gives a cruise fuel mass flow of:

Fuel mass flow (kg/s), mdotf = fc*1.e-2*nofp*wf*Vc/3600=3.33 kg/s

Let us *assume an A380 EINOx of 15g/kg fuel at cruise*, which should be reasonable for the A380, and take as an example an intercontinental flight over the distance: Dc = 10 000 km. The time spent in cruise would then be:

Tc = Dc/Vc = 10000/900 = 11.1 hours = 40 000 s

With the given input the total mass of emitted NOx, mNOx, would become:

mNOx = mdotf*EINOx*Tc = 3.33*15*40e3 = 1 998e3 grams = *2 000 kg (per 10e3km)*

or given as "NOx mass per passenger" and the flight mission over 10 000 km (555 passengers):

mNOx_pp = *3.6 kg/pass (and 10e3km)*

ATLLAS M6T

For the ATLLAS M6T we have a baseline cruise total (air+fuel) mass flow of 1 629 kg/s[18]. Then, with a cruise velocity, Vc, of 1800 m/s the total cruise time for this aircraft would be:

Tc =Dc/Vc = 5 555 s

Starting out with the baseline cruise equivalence ratio ∅ of 0.42 we get a fuel mass flow of:

mdotf = ∅*fs*mdotair = 20 kg/s

and a total mass of NOx (EINOx(∅=0.42)=689 g/kg):

mNOx= mdotf*EINOx*Tc = 20kg/s*0.689kg/kg*5 555s = *76 548 kg (per 10e3km)*

then assuming 200 passengers, the amount per passenger becomes:

mNOx_pp = 382 kg/pass (and 10e3km)

i.e. more than 100 times more NOx per passenger than for the A380 approximation.

Let us then assume that an equivalence ratio of ∅ = 0.25 instead (and still that residential time in combustor is not more than 1 ms). We then reach a smaller fuel flow and EINOx value (31 g/kg according to Table 5), but for the baseline design neither exhaust temperatures nor thrust would be high enough. But let us imagine that after a redesign the resulting thrust would be sufficient for cruise, then the mass of NOx comes out:

mNOx = mdotf*EINOx*Tc = 11.8kg/s*0.031kg/kg*5 555s = *2034 kg (per 10e3km)*

i.e. in line with the A380 approximation. Since the number of passengers is less for the ATLLAS M6T, namely 200, the mass of NOx per passenger for the example flight comes out larger though:

mNOx_pp = 10.2 kg/pass (and 10e3km)

This value indicates a factor 2.5 to 3 times higher NOx emissions per passenger than for the Airbus A380. In case cruise EINOx values of the same order as the A380 (whatever this is) can be reached, the NOx emissions per passenger would be about the same for the two aircraft provided a hydrogen equivalence ratio lower than 0.2 -0.25 can be achieved.

[18] Data in Table 1 is for one out of 4 installed engines of the M6T

In order to reach emissions results at level of the A380 estimate, a further reduction of equivalence ratio or EINOx would be needed based on the M6T baseline data.

Though, as indicated previously, some crucial conditions make the situation more complicated than shown by the previous rather simple outline:

1. First, according to previous discussions, it could be strongly doubted that an EINOx level of 31g/kg would be possible to reach for a M6T at cruise (redesign, more engine power needed, giving higher fuel consumption resulting higher NOx emissions …)
2. Combustion product residential times for the M6T are set to 1 ms, which might be rather short.
3. Emission of NOx at low stratospheric altitudes is considered more critical than at high tropospheric altitudes (though, this area of atmospheric science need to be further explored before definite conclusions could be made in this matter.)
4. Hydrogen is of course superior to kerosene regarding CO_2 and related global warming effects, while it is harder to judge the relative H_20 effects.
5. The fleet of SST:s of the ATLLAS MT6 type would probably never come near the size of a subsonic fleet for intercontinental missions, giving the total fleet NOx emissions smaller even for a cruise EINOx value more than 10 times higher than for a subsonic fleet.

6 Conclusions

The matter of NOx and ozone depletion has been of strong concern for aeronautics and especially for SST's for some decades. There are still open questions regarding atmospheric transport processes and the involved chemistry. The current scientific understanding is though that NOx constitutes the most serious threat coming from aeronautics and tend to destroy ozone in the lower stratosphere, while the opposite effect, a weak ozone gain is found from NOx in the troposphere (near ground this ozone is contributing to the "smog"). While both the ATLLAS M3T and M6T would cruise at altitudes which coincide with the highest ozone concentrations (found around 25 km) the NOx emissions from these aircraft concepts could be considered as crucial. Without considering needed modifications on the studied concepts, a reduction of the cruise altitude would be beneficial regarding NOx.

The current ATLLAS M6T baseline engine inlet conditions make it hard to see an accessible path towards EINOx values of the order of 15g/kg fuel (which is mentioned in literature as a possible future threshold value). Possible "low-NOx" concepts studied, RQL, water injection and the more drastic N_2-O_2 separation, showed only limited and, insufficient NOx reduction starting out from baseline conditions. Based on these ATLLAS studies, either new technology findings that could facilitate combustor residential times of the order of some tenths of milliseconds need to appear, or a re-design that allows for very low equivalence ratios, typically 0.25 or less, resulting in combustion chamber temperatures around 2250K, is needed. If this could be achieved in a general re-design, while keeping combustor residential times as low as a single ms, wEINOx values around 15 g/kg could seam to be possible.

If it was possible for the M6T concept to stay at a cruise equivalence ratio of 0.25 (instead at the baseline value of 0.42) the total amount of emitted NOx at cruise would be of the same order of size as cruise emissions for the A380 for the same flight distance. Since the number of passengers is smaller in the M6T the NOx amount per passenger and distance would be larger than for the A380 with a factor of 2.5 to 3. Not included in this estimate is that thrust actually is estimated to degrade with 45% with this lower ∅, implying that engine power has to be increased a with factor of 1.82 (assuming that the baseline aerodynamic properties are kept). Further, assuming that this needed thrust increase could be reached with a simple addition of engines and fuel, the emitted NOx would increase with the same factor. As a comparison: if the stated baseline ∅ of 0.42 would be needed for a zero net thrust, the NOx emissions/passenger would approximately be 100 times compared with the A380 figures instead of approximately 5 times for the ∅ = 0.25.

The M3T, with its lower working temperature range, has a considerable potential to become a "low-NOx" concept.

References

[1] W.H.Heiser, D.T. Pratt , "Hypersonic Airbrathing Propulsion" AIAA-Education Series 1994 ISBN 1-56347-035-7.

[2] IPCC Special Report: Aviation and the Global Atmosphere, 1999.

[3] R.Sausen et.al. , "Aviation Radiative forcing in 2000: An update on IPCC (1999)", (from the EU-project TRADEOFF) Meteorologische Zeitschrift, Vol. 14, No. 4, 555-561 2005.

[4] IPCC, 4th Assessment Report 2007, WGIIII, Technical summary.

[5] M.R.Raupach et.al, 'Global and regional drivers of accelerating CO_2 emissions' , Proceedings of the National Academy of Sciences , Vol.104, No.24, June 12 2007. Link (17 Nov 2010): http://www.pnas.org/content/104/24/10288.full.pdf+html?sid=efdde1bf-c09d-441e-b3ac-88456f8dd6d5

[6] A. Jones, et.al., "Evolution of stratospheric ozone and water vapour time series studied with satellite measurements" Atmos. Chem. Phys., 9, 6055–6075, 2009.

[7] A. R. Ravishankara et.al , "Nitrous Oxide (N2O): The Dominant Ozone-Depleting Substance Emitted in the 21st Century " , Science Oct. 2 2009Vol. 326 no. 5949 Link (17 Nov 2010): http://www.sciencemag.org/content/326/5949/123.full

[8] CCPO "Stratospheric ozone – an electronic textbook", Link (17 Nov 2010): http://www.ccpo.odu.edu/~lizsmith/SEES/ozone/class/Chap_1/index.htm

[9] "The Atmospheric effects of Stratospheric Aircraft project", National Academy press 1998 Link (17 Nov 2010): http://books.nap.edu/openbook.php?record_id=6255&page=23

[10] M. Dutta et.al. "Parametric Analyses of Potential Effects on Stratospheric and Tropospheric Ozone Chemistry by a Fleet of Supersonic Business Jets Projected in a 2020 Atmosphere", NASA-Report, NASA/CR—2004-213306, October 2004.

[11] V.Grewe "Estimates of the Climate Impact of Future Small-Scale Supersonic Transport Aircraft – Results from the HISAC EU-Project" 2009 (to be presented in "The Aeronautical Journal").

[12] "Nitrogen OxidesWhy and How they are controlled" Technical Bulletin EPA 456/F-99-006R 1999, Link (17 Nov 2010): www.epa.gov/ttn/catc/dir1/fNOxdoc.pdf

[13] U.S. Environmental Protection Agency (EPA); EPA website Link (17 Nov 2010): http://www.epa.gov/air/ozonepollution

[14] G.Hesselman et.al. , "What are the main NOx formation processes in combustion plant?" from the IFRF Online Combustion Handbook 2001, ISSN 1607-9116, Link (17 Nov 2010): http://www.handbook.ifrf.net/handbook/

[15] D.M. Dramlic et.al., "Control and Reduction of Nitrogen in Combustion processes", Journal of Environmental Protection and Ecology 3, no.2 2002.

[16] CAEP 7th MEETING Montreal 5 to 16 February 2007 , "Report of the Independent Experts on the 2006 NOx Review and the Establishment of Medium and Long Term Technology Goals for NOx", Agenda Item 1: Review of proposals relating to aircraft engine emissions, including the amendment of Annex 16, Volume II.

[17] P. Newton, "Long Term Technology Goals for NOx ", Presentation at ICAO website. Link (17 Nov 2010): http://www.icao.int/icao/en/env/LongTermTechnologyGoals.pdf

[18] ICAO Engine Emissions Databank
Link (17 Nov 2010): http://www.caa.co.uk/default.aspx?catid=702&pagetype=90

[19] P. Madden ICAO CEAP presentation: "Supersonic Engine Technology and Work by the Committee on Aviation Environmental Protection (CAEP)", Link (17 Nov 2010): http://www.iae.damtp.cam.ac.uk/meetings/scenic/SCENICpaulmadden.pdf

[20] ICAO CAEP 7th meeting Information Paper : "Correlation Between LTO NOx and Cruise/Climb NOx" 2007.
Link (17 Nov 2010): http://www.tc.gc.ca/media/documents/ac-opssvs/caep7_ip05.pdf

[21] J. Moran ,"Engine Technology Development to Address Local Air Quality Concerns", Presentation at ICAO Colloquium on Aviation Emissions with Exhibition, 14-16 May 2007, Link (17 Nov 2010): http://www.icao.int/envclq/CLQ07/Presentations/moran.pdf

[22] J.Steelant ESA-ESTEC, "Sustained Hypersonic Flight in Europe: Technology Drivers for LAPCATII ", 16th AIAA/DLR/DGLR International Space Planes and Hypersonic Systems and Technologies Conference 16-22 October 2009.

[23] J. Sabnis Pratt & Whitney, "Green Engine Developments for Next Generation Aircraft UC Davis Symposium Aviation Noise and Air Quality San Francisco, California" 2007
Link (17 Nov 2010):
http://airquality.ucdavis.edu/pages/events/2007/aviation_presentations/Sabnis.pdf

[24] H.J. Bauer ,"NOx Emissions from Aeroengines and their Abatement", presentation at Int. Colloquium on Airport Air Quality, Manchester 12 April 2007.
Link (17 Nov 2010): www.cate.mmu.ac.uk/saaq/presentations/Bauer.pdf

[25] EU-Project HISAC, Link (17 Nov 2010): http://www.hisacproject.com/index.html

[26] D.L.Dagget , "Water Misting and Injection of Commercial Aircraft Engines to Reduce Airport NOx" NASA/CR-2004-212957 2004 .
Link (17 Nov 2010): http://gltrs.grc.nasa.gov/reports/2004/CR-2004-212957.pdf

[27] V.Balepin et.al ,"NOx Emission Reduction in Commercial Jets Through Water Injection", NASA TM-2002-2118978, 2002.
Link (17 Nov 2010): http://gltrs.grc.nasa.gov/reports/2002/TM-2002-211978.pdf

[28] D.L.Dagget et al., "Water Injection—Could it Reduce Airplane Maintenance Costs and Airport Emissions?" NASA TM-2007-213652, 2007.
Link (17 Nov 2010): http://gltrs.grc.nasa.gov/reports/2007/TM-2007-213652.pdf

[29] F.H. Holcomb et al. ,"Ramgen Power Systems for Military Engine Applications", ERDC/CERL TR-07-14 2007 Link (17 Nov 2010): http://www.dtic.mil/cgi-bin/GetTRDoc?Location=U2&doc=GetTRDoc.pdf&AD=ADA478293

[30] D. L. Straub et al. "Assessment of Rich-Burn, Quick-Mix, Lean-Burn Trapped Vortex Combustor for Stationary Gas Turbines" , Journal of Engineering for Gas Turbines and Power , Jan. 2005 Vol. 127, Issue 1.

[31] J.Brand et al., "Potential use of hydrogen in Air Propulsion" , AIAA/ICAS International Air and Space Symposium and Exposition: The Next 100 Y 14-17 July 2003, Dayton, Ohio.

[32] "Regulators Guide to Permitting Hydrogen Technologies" U.S. Department of Energy – Energy Efficiency and Renewable Energy, Version 1.0 PNNL-14518 Released 1/12/2004 Link (17 Nov 2010): http://www.pnl.gov/fuelcells/docs/permit-guides/overview_final.pdf

[33] A.M. Crocker et al. , "Progress on Alchemist ACES: Technology for Next Generation Space Transportation", A.M. Crocker et al. AIAA 39th Joint Propulsion Conference Huntsville Alabama 20-23 July 2003.

[34] D.Bizzarri et al., "Propulsion Vehicle integration for Reusable Launcher Using in-Flight Oxygen Collection", Aerospace Science and Technology Vol.12 Issue 6 Sept. 2008.

[35] Input from Martin Plohr DLR via personal communication with Fredrik Haglind, previously at FOI and in the ATLLAS project, now at Technical University of Denmark.

[36] S.Gordon and B.J.McBride, "Computer Program for Calculation of Complex Chemical Equilibrium Compositions and Application" NASA Reference Publication 1311, 1994.

[37] W.H.Heiser, D.T. Pratt , "HAP-code", Code delivered with the textbook: "Hypersonic Airbrathing Propulsion" [1].

[38] J.C. Ianni, Kintecus code ,Windows Version 3.95, 2008 Link (17 Nov 2010): http://www.kintecus.com

[39] A. Lang, M. Sippel, J. Klevanski, U. Atanassov , ATLLAS D2.3.4 Turbo-RAM jet propulsion data set.Technical note: *M6 propulsion data set, CAD model, mass estimation and trajectory analysis.* 2010.

[40] Aerospaceweb.org, Link (17 Nov 2010): http://www.aerospaceweb.org/aircraft/jetliner/a380/

[41] Airbus.com, Link (17 Nov 2010): http://web.archive.org/web/20071214144443/http://www.airbus.com/en/myairbus/airbusview/the_a380_the_future_of_flying.html (originally at: http://www.airbus.com/)

[42] C.J. Jachimowski "An Analytical Study of the Hydrogen-Air Reaction Mechanism With Application to Scramjet Combustion", NASA Technical paper 2791, 1988.

[43] A. Murty Kanury, "Introduction to Combustion Phenomena", Gordon and Breach Science Publishers 1984, ISBN 0-677-02690-0.

FOI, Swedish Defence Research Agency, is a mainly assignment-funded agency under the Ministry of Defence. The core activities are research, method and technology development, as well as studies conducted in the interests of Swedish defence and the safety and security of society. The organisation employs approximately 1000 personnel of whom about 800 are scientists. This makes FOI Sweden's largest research institute. FOI gives its customers access to leading-edge expertise in a large number of fields such as security policy studies, defence and security related analyses, the assessment of various types of threat, systems for control and management of crises, protection against and management of hazardous substances, IT security and the potential offered by new sensors.

FOI
Defence Research Agency
Defence & Security,
Systems and Technology
SE-164 90 Stockholm

Phone: +46 8 555 030 00

Fax: +46 8 555 031 00

www.foi.se